

DEPARTMENT OF OPTICS
FACULTY OF SCIENCE
PALACKY UNIVERSITY OLOMOUC



PhD THESIS

**Quantum Optical Methods
for Communication and Processing
of Information**

Miroslav Gavenda

Supervisor: Doc. Mgr. Radim Filip, Ph.D.

*Submitted in partial fulfillment of the requirements
of the degree of Doctor of Philosophy*

Olomouc, November 15, 2011



Dedicated to my mother



Declaration

This is to certify that:

- (i) All theoretical parts of this thesis described in chapters 4, 5, 6 is the original work of me and my supervisor Radim Filip,
- (ii) the experimental part described in chapter 5 has been performed by experimentalists Fabio Sciarrino, Eleonora Nagali and Francesco De Martini at the La Sapienza University of Rome in Italy. I was collaborating on the proposal of the experimental setup and on the analysis of the experimental data,
- (iii) the experiment described in chapter 6 has been performed by experimentalists Lucie Čelechovská, Jan Soubusta and Miloslav Dušek at the Palacky University Olomouc in the Czech Republic. I was collaborating on the proposal of experimental setup and on the analysis of the experimental data,
- (iv) due acknowledgement has been made in the text to all other material used.

Miroslav Gavenda



Curriculum Vitae

- Name: Miroslav Gavenda
- Date of Birth: November 14, 1977
- Nationality: Czech
- Education:
 - 1998-2001: BSc student of optics and optoelectronics, Faculty of Science, Palacky University, Olomouc, Czech Rep., received academic title BSc
 - 2002-2003: Exchange student at Department of Physics, Umea University, Sweden
 - 2003-2004: MSc student of optics and optoelectronics, Faculty of Science, Palacky University, Olomouc, Czech Rep., received academic title MSc
 - 2004 - : PhD student of optics and optoelectronics at Dept. of Optics, Faculty of Science, Palacky University, Olomouc, Czech Rep.
- Working experience:
 - From April 1, 2006 employed at the Dept. of Optics, Faculty of Science, Palacky University, Olomouc as a junior researcher
- Research interests:
 - Quantum optics, physics of quantum information, numerical methods in physics
- Scientific stays:
 - September 8, 2005 - October 8, 2005: 1 month stay at the Max-Planck Institute for Science of Light, Erlangen, Germany
 - June 16, 2011 - September 13, 2011: 3 months stay at the Institute for Quantum Information Science at the University of Calgary, Calgary, Canada
- Participation as a member in following research projects:
 - 2006-2011: research project "Centre of Modern Optics" No. LC06007 of the Ministry of Education of the Czech Republic
 - 2008-2010: research grant "Electro-optical control of quantum noise of light" No. 202/08/0224 of the Grant Agency of the Czech Republic
 - 2011-2013: project "International Centre for Information and Uncertainty" No. CZ.1.07/2.3.00/20.0060 of the European Social Fund and Ministry of Education of the Czech Republic



Publications

During the course of this project, a number of public presentations have been made which are based on the work presented in this thesis.

- **M. Gavenda, L. Čelechovská, J. Soubusta, M. Dušek, R. Filip**, *Visibility bound caused by a distinguishable noise particle*, Phys. Rev. A 83, 042320 (2011).
- **M. Gavenda, R. Filip, E. Nagali, F. Sciarrino, and F. De Martini**, *Complete analysis of measurement-induced entanglement localization on a three-photon system*, Phys. Rev. A 81, 022313 (2010).
- **E. Nagali, F. Sciarrino, F. De Martini, M. Gavenda, and R. Filip**, *Entanglement Concentration After a Multi-Interactions Channel*, Adv. Sci. Lett. 2, 448-454 (2009).
- **F. Sciarrino, E. Nagali, F. De Martini, M. Gavenda, and R. Filip**, *Entanglement localization after coupling to an incoherent noisy system*, Phys. Rev. A 79, 060304 (2009).
- **M. Gavenda and R. Filip**, *Quantum adaptation of noisy channels*, Phys. Rev. A 78, 052322 (2008).



Acknowledgements

First of all I would like to thank my supervisor, colleague but mainly a friend Radim Filip who introduced me the world of science, gave me a direction in research and supported me during my phd studies.

I would like to thank also other colleagues from Dept of Optics in Olomouc for collaboration, discussion and advises (in alphabetical order): Lucie Čelechovská, Miloslav Dušek, Jiří Herec, Jaromír Fiurášek, Miroslav Ježek, Petr Marek, Michal Mičuda, Ladislav Mišta, Vladyslav Usenko.

Special thanks belongs to experimentalists Fabio Sciarrino and Eleonora Nagali from the La Sapienza University of Rome for a succesful collaboration.

Continuous thank belongs to my wife Kateřina who tolerated my bad days and to my daughter Marie that she is.



Introduction

Physics of quantum information brings ideas from quantum physics, mathematics and computer science in order to do tasks impossible within laws of classical physics: fast computation beyond the classical level, unconditionally secure distribution of cryptographic key, teleportation of states to briefly mention a few of them.

Since the born of quantum information in the 80's of the nineteenth century the discipline evolved into a quite mature state. It has been proposed many quantum protocols and many of them were successfully experimentally tested. Quantum key distribution has been even transformed into commercially available products.

Many quantum protocols are based on the coherent superposition of quantum states or use as a resource entangled states. These resources are however subject to environment that causes reduction or even loss of them. The problem of keeping the quantum resources robust or less vulnerable to environment is of huge importance in quantum communication and processing of information.

This PhD thesis contributes to the problem of loss of quantum entanglement with two new protocols that are able in some particular cases recover lost entanglement, and further contributes to the problem of decoherence where uncovered a role of distinguishability in the process of decoherence.



Contents

I	Background	1
1	State of the Art	3
2	Goals of the thesis	9
3	Methods and Tools	13
3.1	Quantum states	13
3.1.1	Pure states	13
3.1.2	Mixed states	14
3.1.3	Evolution of quantum states	15
3.1.4	Composite systems	15
3.1.5	Quantum measurement	16
3.2	Quantum channels	17
3.2.1	Physical motivation	17
3.2.2	Representations of quantum channel	18
3.2.3	Quantum filters	19
3.2.4	Examples of quantum channels	20
3.3	Quantum entanglement	21
3.3.1	Entanglement of bipartite states	22
3.3.2	Bell inequalities	23
3.3.3	Entanglement measures	24
3.3.4	Entanglement of multipartite states	27
3.4	Decoherence and evolution of entanglement	28
3.4.1	Decoherence	28
3.4.2	Evolution of entanglement	30
3.5	Numerical methods	31
3.6	Experimental methods and techniques	33

II	Research Work	35
4	Adaptation of Quantum Channels	37
4.1	Introduction	37
4.2	Quantum Adaptation of Independent channels	39
4.3	Asymmetrical example	42
4.4	Symmetrical example	46
4.5	Conclusion	48
5	Entanglement localization	49
5.1	Introduction	49
5.2	Theory	51
5.2.1	Coherent coupling	51
5.2.2	Partially incoherent coupling	55
5.3	Experimental Implementation	61
5.3.1	Experimental setup	61
5.3.2	Incoherent coupling	64
5.3.3	Coherent coupling	68
5.3.4	Mixture of coherent and incoherent coupling	70
5.4	Appendix	72
5.4.1	Coherent coupling	72
5.4.2	Incoherent coupling	74
5.5	Conclusion	76
6	Particle distinguishability and decoherence	79
6.1	Theoretical framework	79
6.2	Experimental implementation	84
6.3	Results	85
6.4	Conclusion	86
7	Summary and Outlook	89

Part I

Background

Chapter 1

State of the Art

Quantum physics is still a subject of huge progress after almost 100 years from its foundation. It is mainly caused by development of experimental techniques that are able to manipulate with objects (single photons, atoms, molecules etc.) at the level where the description of physical phenomena by laws of classical physics fails. With such skills we can nowadays set up much more complex and precise experiments to test our theoretical predictions at the fundamental and applied level or even harness the laws of quantum physics in quantum cryptographical systems that became recently commercially available.

Quantum physics lies on a few rather simple principles. One of them, the superposition principle [1], postulates that whenever a quantum state can be found in either one of two states $|\psi_1\rangle$ or $|\psi_2\rangle$, it can also be found in a state $|\psi\rangle$ given by their complex linear combination $|\psi\rangle = c_1|\psi_1\rangle + c_2|\psi_2\rangle$. We call such a superposition of states a coherent one. The coherent superposition of quantum states can be manifested in quantum interference behaviour, where the probability of finding the system in a superposed state $|\psi\rangle$ is not generally given by a sum of the corresponding probabilities of finding the system in state $|\psi_1\rangle$ and $|\psi_2\rangle$. The quantum interference occurs if principal indistinguishability of possible physical states, the quantum system can evolve to, is assured. The coherent superposition of states is not generally allowed in classical physics.

Extending the superposition principle to at least two spatially separated quantum objects may lead to another non-classical phenomena, quantum entanglement. It lies at center of interest of the contemporary quantum physics. Entanglement was first recognized by Schrödinger [2], Einstein, Podolsky and Rosen [3] in 1930's. It is a property of compound quantum systems that are in a very special way correlated (entangled). Imagine two quantum systems labeled a , b such that each of them may be found in orthogonal states $|\psi\rangle$ or $|\psi_\perp\rangle$. According

to superposition principle quantum state $|\Psi_{-}\rangle = (1/\sqrt{2})(|\psi\rangle_a|\psi_{\perp}\rangle_b - |\psi_{\perp}\rangle_a|\psi\rangle_b)$ is also an allowed state, entangled state. Correlation in such states is very unusual and does not have a counterpart within classical physics. Moreover in 1964 John Bell proved that all states that could be explained by local hidden variable theories must satisfy certain inequality - now called Bell inequality [4]. The existence of states violating the Bell inequality shows that certain correlations carried by quantum systems cannot be explained by laws of classical physics. Version of Bell inequality, called CHSH inequality, suitable for experimental testing was introduced here [5]. Many experiments, testing the violation of Bell inequality for such states, were performed which confirmed the violation of Bell inequality as was predicted by quantum theory [6, 7, 8]. The first experiments were build using quantum states of light and the experimental methods of quantum optics.

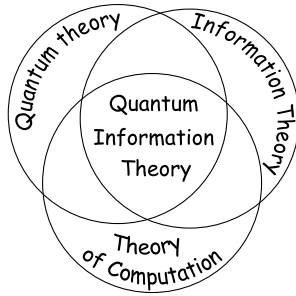


Figure 1.1: The emergence of quantum information theory.

The coherent superposition and entanglement were incorporated as a central notion into a new interdisciplinary domain called quantum information theory (see Fig. 1.1) brings together ideas from the fields of quantum mechanics, theory of information and theory of computation. The two quantum properties play crucial roles in quantum information transfer and processing.

In classical information theory an elementary amount of information carried by a classical system is known as a bit - a two-state object. The system can be either in one state or the other. The classical information processing can be always explained by transformation of bits. Analogously an elementary processing unit in quantum information is called a qubit (quantum bit) - a two-state quantum system. The superposition principle says that a physical system can be found also in complex superposition of basis states of the qubit. Coherent superposition is responsible for enormous amount of parallel processing threads ensuring huge non-classical computational power of a potential quantum computer [9]. The unconditional security of quantum key distribution [10, 11] is based either on complementarity or Bell inequality violation. Entanglement is also a resource for quantum teleportation [12] and quantum dense coding [13] which have been

demonstrated in pioneering experiments involving entangled quantum states of light [14, 15, 16, 17]. Cryptographical systems based on quantum key distribution are today even commercially available [18, 19]. Entanglement is also responsible for efficiency of quantum computation algorithms [9] that are the building blocks of potential quantum computer. Moreover entanglement can help in such tasks as the reduction of classical communication complexity [20], quantum estimation of damping constant [21], frequency standards improvement [22] and clock synchronization [23].

However, many systems cannot preserve quantum properties for long time due to decoherence or/and influence of noise [24, 25]. According to Żurek: “The decoherence is caused by the interaction in which the environment in effect monitors certain observables of the system, destroying coherence between the pointer states corresponding to their eigenvalues”. Quantum superpositions are not treated equally by decoherence. The interaction with the environment singles out the preferred set of states - pointer states, while the other loss their coherence - decohere. Decoherence process leads to environment-induced superselection, *einselection*, which enforces classicality.

Traditional view of quantum decoherence is based on processes which continuously in time lower the coherence between the states of quantum system. The coherence vanishes after an infinite amount of time. We can distinguish two main physical reasons behind such a continuous kind of decoherence. Fluctuations of external macroscopic physical parameters of the system (quantum state) [26] can give rise to decoherence. We call such a decoherence continuous dephasing. Due to fluctuations of the parameters the non-diagonal terms (“phase” terms) of outgoing density matrices decay whereas the diagonal terms representing energy of the system are preserved.

Continuous unitary coupling of the system to the environment is another source of decoherence. The joint state consisting of system and environment becomes entangled due to the coupling. Environmental states monitor the observables of the system leading to destruction of quantum coherence between system states. Decohered states are einselected. That model of decoherence was described in [27, 28] and it was experimentally tested in Ref. [29].

Since the first two mechanisms of decoherence have been already extensively investigated, we have focused our attention to different kind of decoherence mechanism. It is based on mixing quantum particle with other quantum particle representing noise. This model of decoherence shows opposed to the above two mechanisms discrete character. We have considered the microscopic noise, rep-

represented by a single photon emitted by environment and mixed up with signal represented by another single photon (system). Further, no spontaneous emission from the system [30] or collision to the environment appear [31]. Therefore, the only relevant source of decoherence is noise and its distinguishability from the signal. The role of principal distinguishability between “signal” and “noise” photon has been investigated. The coherence of the signal particle is lowered not continuously but by steps proportional to number of noise particles involved. We can recognize an elementary “unit of decoherence” (impact of decoherence) which cannot be divided in time. From the above reasons the decoherence model we describe can be considered as discrete one. The theoretical predictions and experimental test of our model were published in [32].

The decoherence can cause failure of quantum information tasks. Therefore we need to combat the decoherence in order to maintain the quantum superposition of states as a resource in quantum information processing. First method to combat decoherence was introduced in [33]. States of the system were encoded to special states that are immune to system-environment coupling. The procedure was afterwards generalized and is known as a decoherence free subspace method. The states of the system are encoded on subspaces (decoherence free subspaces) of the entire Hilbert space in such a way that the quantum superposition is preserved [34].

Active protection of coherent superpositions are based on quantum control theory and quantum error correction techniques. Doherty et. al. [35] proposed a technique based on POVM measurement and Hamiltonian feedback. Viola et. al. [36] use the technique of dynamical decoupling and control theory to bend the evolution of quantum system. Buscemi et. al. [37] give limits on reversion of quantum decoherence by classical feedback from the environment. The search for protocols for reverting or at least slowing down the process of decoherence is very important for future applications of quantum information processing.

Although scientific interest in entanglement lasts over 30 years the research has focused predominantly on its static properties, its carriers (entangled states), measures and applications. Only recently discovered phenomena called Sudden Death of Entanglement (SDE) turned the attention to the question of dynamical properties of entanglement, its time evolution in noisy environment. Yu and Eberly showed [38] that the entanglement of a pair of non-interacting qubits in the presence of spontaneous emission may decay not exponentially but in finite time. Generally SDE leads to finite time disentanglement of previously entangled quantum state. Due to SDE entanglement completely vanishes and no entangle-

ment can be distilled back - entanglement breaking. Therefore the quantum states leaving entanglement breaking channel cannot serve to its application purpose. Dodd et al. [39] investigated connection between SDE and quantum decoherence. They found that disentanglement occurs after a finite time unlike decoherence which vanishes in a given basis asymptotically. After the discovery of SDE, it has been examined in several distinctive model situations involving pairs of atomic, photonic and spin qubits [40, 41, 42], continuous Gaussian states [43], multiple qubits [44] and spin chains [45]. SDE was also experimentally verified by using entangled photon pairs [46] and atomic ensembles [47]. There was also reported opposite phenomena to the SDE - entanglement sudden birth [44] in particular environments. It shows an oscillatory behaviour of entanglement.

From the current state of research we know that the SDE is a real fundamental problem in quantum physics. It is necessary to avoid or at least delay it in order to provide robust resource for quantum information tasks. Known entanglement enhancement protocols as distillation [48], purification [49] and concentration [50] cannot be exploited for avoiding SDE. The prerequisite for their successful operation is a presence of at least a bit of residual entanglement in input states, but the output states suffering from SDE are no more entangled.

Quantum analog of classical error correction methods have been studied [51] to provide protection against SDE. The method uses the appropriately designed redundancy of the input systems. Unfortunately error correction is very complicated in practice because noisy channels are dynamical systems with not very well predictable behaviour. In [52] we have proposed probabilistic quantum filtering method, quantum adaptation, which can properly adapt sequential consecutive quantum channels in order to avoid SDE. Being able to partially control the channel we have to divide the whole quantum channel into smaller pieces and apply quantum filters which properly matches the quantum channels one to the other. Contrary to distillation procedures to successfully adapt a quantum channel there is no need for residual entanglement leaving the channel. The impossibility to avoid the SDE by protocols acting just on the system of interest lead the researchers to think about active operations jointly on the system of interest and environment. Although the complete inversion of joint system-environment dynamics is practically impossible due to generally very complex dynamical environment, some partial information from the environment can be helpful [53].

In [54] the idea of unlocking of hidden entanglement was presented. There has been estimated that in order to unlock the hidden entanglement from a separable

mixed state of two subsystems an additional bit or bits of classical information is needed. The classical information determines which entangled state is actually present in the mixture. However no strategy was presented in order to extract this information from the system of interest or the environment.

In [55] Yamamoto et al. used the concept of measurement feedback control to avoid SDE in a quantum network consisted of two distantly separated cavities connected via one-way optical field. The method uses a direct measurement on one cavity followed by back control of both of them.

Other methods use dynamic manipulation such as mode modulation [56] or the quantum Zeno effect [57].

In [58, 59] we have shown that entanglement lost in particular SDE channel can be localized [60] back for the further application just by performing suitable measurement on the surrounding system and the proper feed-forward quantum correction. The measurement and feed-forward operation substitute, at least partially, a full inversion of the coupling. That requires to keep very precise interference with the surrounding systems.

Although above methods show "way to go", the issue of how to avoid SDE-type decorrelation in a realistic physical system is incompletely resolved at this time and requires further research. For review on SDE see [61].

Chapter 2

Goals of the thesis

During the course of my phd studies we found several open problems in quantum information that were worth to study.

- I already mentioned that environment inevitably couples to our state of interest and may lead to decrease of entanglement. It is well known that quantum entanglement can be even lost in some quantum channels. Such a behaviour, called sudden death of entanglement, generally give rise to malfunction of quantum protocols. It is natural to ask how to avert the loss of entanglement. We cannot combat the total loss of entanglement with the usual techniques such as quantum distillation, purification or concentration because the necessary prerequisite for such a protocols to be successful is that the state posses at least a bit of quantum entanglement. Strategy different from the usual one has to be implemented. One of the goals of this thesis is to propose a protocol that would deal with the problem of sudden death of entanglement. The protocol must inevitably works with the intestines of quantum channel or with the environment it couples to. Our goal is to find simple protocol that would achieve the task not for a general quantum channel but rather to verify on simple examples that the principles of the methods work. We will investigate two different approaches with the relation to the above problem.
 - The goal in this approach is to divide the entanglement breaking channel into a shorter pieces, which are no more entanglement breaking. Between the adjacent quantum channels propose probabilistic quantum filtering to properly adapt the channels so that the whole sequence of channels is again entanglement preserving (see Fig. 2.1 and 2.2).
 - If the previous approach (adaptation) is not enough or suitable for combating the SDE, the goal is to propose new protocol that would

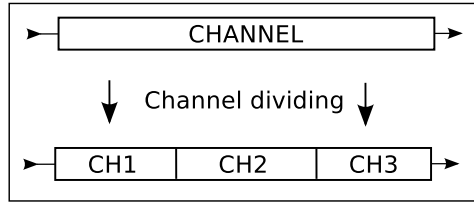


Figure 2.1: Division of channel

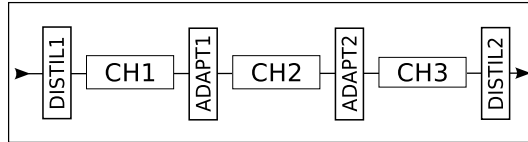


Figure 2.2: Adaptation of channel

work actively with environment. In this case the quantum channel is not described as a black box connecting input and output quantum states but this time the structure of the environment is stressed (see Fig. 2.3). Obviously we cannot usually control the whole environment of the system of interest but since the part of environment predominantly responsible for the dynamics of the state of interest is much smaller we could deal with it. Therefore the relevant and accessible part of the environment can be measured and afterwards a proper feed-forward quantum correction may be applied to the outgoing state, we call the protocol quantum localization. An experimental proposal that would test the theoretical predictions of quantum localization is also desirable.

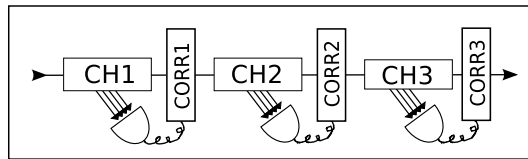


Figure 2.3: Environment measurement and quantum correction

- The controlled behaviour of quantum systems in coherent superpositions is nowadays a central issue in the quantum information business. In order to have the systems under such control we must avoid the decoherence. The decoherence process can have several reasons: It can arise from fluctuations of the external macroscopic parameters, it can appear as the result of coherent coupling between the system and the environment or it can be evoked by mixing the system with some other system representing noise.

- The previous approaches raise the question if there exist an elementary decoherence process lowering the coherence of the system by a discrete amount. Such decoherence unit cannot be further divided and its correction is possible by detection of environment only. The aim is to investigate decoherence process based on mixing system and noise particle which depends on principal distinguishability between them only and observe its discrete nature (see Fig. 2.4). To focus on the process under our interest, it is necessary that no fluctuations of physical parameters, collisions of particles and no emissions from environment or system appear. Even presence of such additional (partly) distinguishable system can cause decoherence of the system of interest. The goal is to propose a simple quantum interferometric model where we could uncover such a type of decoherence, calculate theoretical predictions, propose an experimental setup and perform an experimental verification with a collaboration of quantum optical laboratory.

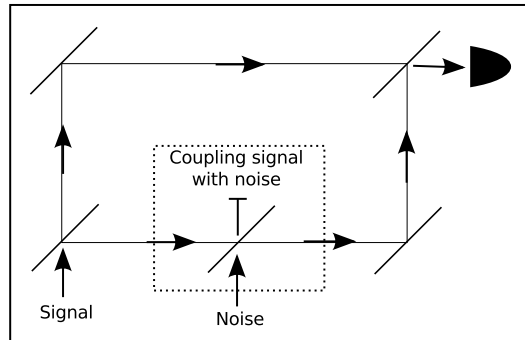


Figure 2.4: Mixing signal and noise particle in an interferometer

Chapter 3

Methods and Tools

3.1 Quantum states

3.1.1 Pure states

The concept of state of physical system is in quantum theory more stressed than in classical theories. In classical deterministic theories the physical state is assigned to individual systems whereas the probabilistic nature of quantum mechanics force us to use the notion of (quantum) ensembles. In [1] state space and states are postulated by following expression: “To any isolated physical system is associated a complex vector space V with inner product (Hilbert space) also called state space. The system is completely described by unit vector in the system’s space.” Such defined quantum state is called pure and mathematically is expressed in Dirac notation by a vector $|\psi\rangle$, called ket vector, in state space V . The inner product of vectors $|\phi\rangle$ and $|\psi\rangle$ is a function $(|\phi\rangle, |\psi\rangle)$ from $V \times V$ to \mathbb{C} satisfying the usual requirements from the theory of vector spaces [62]. Algebraic dual space V^d to the space V is a set of linear functionals from V to \mathbb{C} with definition of adding and multiplication via inner product:

$$(c\langle v| + \langle w|)(|\psi\rangle) = c(v, \psi) + (w, \psi), \quad (3.1)$$

Vectors from V^d are called dual vectors and in Dirac notation are labeled by bra vector $\langle\psi|$. The inner product of two vectors $|\phi\rangle, |\psi\rangle$ in Dirac notation is labeled by $\langle\phi|\psi\rangle$ and its particular definition depends on the type of vector space we work with.

Superposition postulate of quantum mechanics says that if a quantum system can be found in a quantum state given by a vector $|\psi_1\rangle$ or by a vector $|\psi_2\rangle$ then it can be also found in a complex coherent superposition of the two states $|\psi\rangle$

given by

$$|\psi\rangle = a|\psi_1\rangle + b|\psi_2\rangle, \quad (3.2)$$

where a, b are complex numbers.

The simple example of a quantum system is a system with two dimensional state space, called *qubit* (quantum bit):

$$|\psi\rangle = a|H\rangle + b|V\rangle, \quad (3.3)$$

where $|H\rangle = [0, 1]^T$, $|V\rangle = [1, 0]^T$ are two-dimensional basis (column) vectors representing e.g. the polarization state of a photon (horizontal and vertical) and a, b being complex numbers satisfying normalization condition $|a|^2 + |b|^2 = 1$. We can then represent any polarized state of a photon giving the proper a, b . The inner product in space of qubits is given just by scalar product of two vectors $\langle\phi| = c\langle H| + d\langle V| = [c, d]^T$, $|\psi\rangle = a|H\rangle + b|V\rangle = [a, b]^T$ in \mathbb{C}^2 :

$$\begin{aligned} \langle\phi|\psi\rangle &= (c^*\langle H| + d^*\langle V|)(a|H\rangle + b|V\rangle) = \\ &= c^*a\langle H|H\rangle + c^*b\langle H|V\rangle + d^*a\langle V|H\rangle + d^*b\langle V|V\rangle = c^*a + d^*b \end{aligned} \quad (3.4)$$

$$\langle\phi|\psi\rangle = [c^*, d^*] \cdot [a, b]^T = c^*a + d^*b, \quad (3.5)$$

where the orthonormality of the basis vectors $|H\rangle, |V\rangle$ was used ($\langle H|H\rangle = \langle V|V\rangle = 1, \langle H|V\rangle = \langle V|H\rangle = 0$) and the dual vector (row vector) is created by transposition and complex conjugation from the state space vector: $\langle\phi| = ((|\phi\rangle)^T)^* = (([c, d]^T)^T)^* = [c^*, d^*]$.

3.1.2 Mixed states

Pure state is just a mathematical fiction that cannot describe the physical reality because it is experimentally impossible to prepare an ensemble of precisely the same states. What we can just know is the probability p_i that our system is in a pure state $|\psi_i\rangle$. The whole ensemble of such states, the system could be in, is called a mixed quantum state and mathematically may be expressed by a density matrix

$$\rho = \sum_i p_i |\psi_i\rangle\langle\psi_i|. \quad (3.6)$$

It is a convex sum of pure states $|\psi_i\rangle$ the quantum system may be in with a natural condition that $\sum_i p_i = 1$. The transition from mixed states to more mixed states is a result of decoherence.

E.g. the general mixed state of a qubit ρ can be represented by 2×2 matrix

in Bloch's form:

$$\rho = \frac{\mathbb{1} + \vec{m} \cdot \vec{\sigma}}{2}, \quad (3.7)$$

where $\vec{m} \in \mathbb{R}^3$, $\|\vec{m}\| \leq 1$ and $\vec{\sigma}$ is a vector of matrices $\vec{\sigma} = [\sigma_1, \sigma_2, \sigma_3]$ and σ_j are the Pauli matrices

$$\sigma_1 = \begin{pmatrix} 0 & 1 \\ 1 & 0 \end{pmatrix}, \quad \sigma_2 = \begin{pmatrix} 0 & -i \\ i & 0 \end{pmatrix}, \quad \sigma_3 = \begin{pmatrix} 1 & 0 \\ 0 & -1 \end{pmatrix}. \quad (3.8)$$

The decoherence can be here visualize by the purity $P = \text{Tr}[\rho^2]$ of the mixed state ρ . The purity is equal to one for pure qubits and 1/2 for completely mixed qubits. When pure qubit is subject to decoherence process its purity is lowered from the unit value for pure state to value 1/2 for completely mixed state.

3.1.3 Evolution of quantum states

The time evolution of a quantum state $|\psi\rangle$ resp. ρ of a closed quantum system evolves unitarily between times t_1 and t_2 according to

$$|\psi(t_2)\rangle = U(t_2, t_1)|\psi(t_1)\rangle \quad \text{resp.} \quad \rho(t_2) = U(t_2, t_1)\rho(t_1)U(t_2, t_1)^\dagger \quad (3.9)$$

where $U(t_2, t_1)$ is a unitary operator ($U(t_2, t_1)U(t_2, t_1)^\dagger = \mathbb{1}$), called propagator (evolution operator), satisfying a composition property $U(t_2, t_0) = U(t_2, t_1)U(t_1, t_0)$. From the evolution postulate we can derive the famous Schrödinger equation:

$$i\hbar \frac{d}{dt}|\psi\rangle = H|\psi\rangle, \quad (3.10)$$

where \hbar is Plank's constant, H is Hamiltonian operator of the system. The extension of evolution postulate involving density matrices is straightforward

$$i\dot{\rho}(t) = [H(t), \rho(t)]. \quad (3.11)$$

3.1.4 Composite systems

To model decoherence process based on coupling with environment we need to deal with compound quantum states made from composition of other quantum states. The state space of a composite physical system \mathcal{H} is a tensor product $\mathcal{H} = \mathcal{H}_A \otimes \mathcal{H}_B$ of the state spaces \mathcal{H}_A , \mathcal{H}_B of its components A , B .

A joint physical system with density matrix ρ of two at most classically correlated systems A and B described by their density matrices ρ_A and ρ_B is

given by tensor product

$$\rho = \rho_A \otimes \rho_B \quad (3.12)$$

The structure of possible states of composite space $\mathcal{H}_A \otimes \mathcal{H}_B$ is much more richer and involves also correlated states that cannot be written by the form of (3.12) - entangled states. The system A may label e.g. the system of interest and the system B environment.

E.g. the most general density matrix of two-qubits can be expressed in the following form

$$\rho_{AB} = \frac{1}{4} \left(\mathbb{1} \otimes \mathbb{1} + \sum_{j=1}^3 \mathbb{1} \otimes m_j \sigma_j + \sum_{j=1}^3 \sigma_j n_j \otimes \mathbb{1} + \sum_{i=1}^3 \sum_{j=1}^3 t_{ij} \sigma_i \otimes \sigma_j \right), \quad (3.13)$$

where $(m_1, m_2, m_3) \in \mathbb{R}^3$, $(n_1, n_2, n_3) \in \mathbb{R}^3$ and t_{ij} are elements of 3×3 real matrix called correlation matrix.

3.1.5 Quantum measurement

The quantum measurement is a physical process described by set $\{M_j\}$ of measurement operators acting on states of the quantum system. If the system is in a pure state $|\psi\rangle$ than the probability of getting the result j of the measurement is

$$p_j = \langle \psi | M_j^\dagger M_j | \psi \rangle, \quad (3.14)$$

where $\sum_j M_j^\dagger M_j = \mathbb{1}$ and the state of the system after the measurement is

$$\frac{M_j |\psi\rangle}{\sqrt{p_j}} \quad (3.15)$$

If the measurement operator is a projector ($M_i M_j = M_i \delta_{ij}$) then such a measurement is called projective measurement or von Neumann measurement. A more general class of measurements is allowed in quantum mechanics. Noticing that the operator $M^\dagger M$ in the formula (3.14) is positive we can replace it by some positive operator E_j with condition $\sum_j E_j = \mathbb{1}$. Then such a set of operators are called POVM elements from “positive operator-valued measure” and measurement is POVM measurement or generalized measurement. There exist a square root of the operator $\sqrt{E_j} = B_j$ for any positive operator E_j defined by $E_j = B_j^2$. We can then define measurement operators similar to the case of projectors above by $M_j = \sqrt{E_j}$.

We can extend the description of the quantum measurement to mixed states

by density matrix approach. Suppose we measure quantum state ρ by measurement operators M_j then we get the result j with probability of success

$$p_j = \text{Tr}[\rho M_j^\dagger M_j] \quad (3.16)$$

and the state ρ collapses to the state ρ_j

$$\rho_j = \frac{M_j \rho M_j^\dagger}{p_j} \quad (3.17)$$

Measurement on a subsystem \mathcal{H}_B of a composite system $\mathcal{H}_A \otimes \mathcal{H}_B$ is represented by a tensor product of measurement operators M_j^B on the subsystem B and identity operator $\mathbb{1}_A$ on subsystem A

$$M_j = \mathbb{1}_A \otimes M_j^B. \quad (3.18)$$

After the measurement we can trace out over the subsystem B (it can represent e.g. environment) and get the state ρ_j^A of a subsystem A conditioned on the result j of a measurement on the subsystem B (environment).

$$\rho_j^A = \text{Tr}_B[M_j \rho^{AB}] = \text{Tr}_B[(\mathbb{1}_A \otimes M_j^B) \rho^{AB}] \quad (3.19)$$

3.2 Quantum channels

3.2.1 Physical motivation

Throughout the thesis we successfully use the concept of quantum channel. Quantum channel is a physical map that takes as an input density matrix of a state of interest and produces as an output generally different density matrix. It can be represented in various mathematical forms. Which representation to use depends on the particular problem we solve.

The physical picture behind the quantum channel is rather straightforward. Imagine at input a quantum state of our interest represented by its density matrix ρ . State ρ is always surrounded by some other system, called usually environment, and assign it density matrix σ . Supposing that the two states are initially non-correlated its compound state can be described by tensor product of the two states $\rho \otimes \sigma$. According to the evolution postulate of quantum mechanics a quantum state of a closed system evolves unitarily via an unitary operation U . Therefore applying that unitary transform to our compound system we get at the output

following state $U(\rho \otimes \sigma)U^\dagger$. Since we are interested in the state of the system at the output we shall perform tracing operation over the environmental state. We may summarize the action of a quantum channel Φ by following expression called an environmental model of quantum channel:

$$\Phi(\rho) = \text{Tr}_2 [U(\rho \otimes \sigma)U^\dagger], \quad (3.20)$$

where I generalized the map with assumption of $\text{Tr} [\Phi(\rho)] \leq 1$, the probability of success of the operation (quantum channel) may be less than or equal to one.

3.2.2 Representations of quantum channel

Environmental model

We have described the environmental model of a quantum channel in the previous subsection and the model is represented by the formula (3.20).

Kraus form

From the mathematical point of view the quantum channel is a completely positive trace decreasing map and Kraus has shown that such a map is of the form:

$$\Phi(\rho) = \sum_i A_i \rho A_i^\dagger, \quad (3.21)$$

where A_i are operation elements or Kraus operators, satisfying $\sum_i A_i^\dagger A_i \leq \mathbb{1}$. Moreover if no loss of particle appears the map Φ is a trace preserving with $\sum_i A_i^\dagger A_i = \mathbb{1}$ and the output of the channel is again a density matrix (the operation is deterministic)

$$\rho' = \Phi(\rho). \quad (3.22)$$

We call the (3.21) form the Kraus representation or operator-sum representation.

Affine maps

We found useful a representation of qubit quantum channels by affine maps. If a qubit is described in a Bloch's form by density matrix $\rho = \frac{1}{2}(\mathbb{1} + \vec{m} \cdot \vec{\sigma})$ then the action of the quantum channel may be represented by an affine map

$$\Phi(\rho) = \frac{1}{2}(\mathbb{1} + (\hat{T}\vec{m} + \vec{t}) \cdot \vec{\sigma}), \quad (3.23)$$

where \hat{T} is a 3×3 real matrix and \vec{t} is 3D vector. The Bloch's vector of the state is changed from \vec{m} to $\hat{T}\vec{m} + \vec{t}$.

Jamiołkowski isomorphism

Very useful in dealing with quantum channels is a relation between quantum states and quantum channels. The quantum channel Φ can be represented as a quantum state ρ_Φ in a larger space via so called Jamiołkowski isomorphism. It uses an action of the map Φ on a part of the maximally entangled state $|\Psi_-\rangle$:

$$\rho_\Phi = (\Phi \otimes \mathbb{1})(|\Psi_-\rangle\langle\Psi_-|) \quad (3.24)$$

3.2.3 Quantum filters

An example of a trace decreasing quantum map is a quantum filter. It is a probabilistic operator applied on a quantum state represented by a density matrix ρ to produce another quantum state represented by a density matrix ρ' . The performance of the quantum filter can be described by the transformation

$$\rho' = \frac{F\rho F^\dagger}{\text{Tr}(F\rho F^\dagger)} \quad (3.25)$$

where F is quantum operation (filter) that can be decomposed into $F = UF_0V$, where U, V are single-qubit unitary operations and $F_0 = \text{diag}(1, \sqrt{r})$ with $0 \leq r \leq 1$. The term $\text{Tr}(F\rho F^\dagger)$ gives the probability of success of the filter F .

Single-copy distillation procedure involving filtration operations was used by Verstraete et. al. in [63, 64] to concentrate entanglement up to states with maximal possible violation of CHSH Bell inequality. They found that entanglement of formation, concurrence, negativity, fidelity and the CHSH-violation of a mixed state ρ are all maximized under the same stochastical local filtering operations (SLOCC). These operations bring the state ρ into a state diagonal in the Bell basis.

Multi-copy distillation protocols were found which can asymptotically bring any two-qubit entangled state to the maximally entangled two-qubit state [65, 66, 67]. The usage of Bell diagonal states in multi-copy distillation protocols were shown here [68].

3.2.4 Examples of quantum channels

Unital channels

Important class of quantum channels consists of unital quantum channels or doubly-stochastic channels. Quantum channel is unital if it maps an identity operator to itself:

$$\Phi(\mathbb{1}) = \mathbb{1}. \quad (3.26)$$

The unital quantum channel leaves the maximally mixed state intact.

Depolarizing channel

Suppose we have a qubit ρ which is with probability $1 - p$ totally depolarized (replaced by a completely mixed state) and with probability p is left untouched. Then the quantum channel, called depolarizing channel, is expressed by following equation:

$$\Phi(\rho) = p\rho + \frac{1-p}{2}\mathbb{1} \quad (3.27)$$

The corresponding Kraus operators for the depolarizing channel are

$$A_0 = \sqrt{\frac{1+3p}{4}}\mathbb{1}, \quad A_i = \sqrt{\frac{1-p}{4}}\sigma_i, \quad (3.28)$$

where $i = 1, 2, 3$ and σ_i being the Pauli matrices.

When one qubit from the maximally entangled state of two qubits $|\Psi_-\rangle$ (singlet) passes the depolarizing channel, we get at the output Werner state

$$p|\Psi_-\rangle\langle\Psi_-| + \frac{(1-p)}{4}\mathbb{1} \otimes \mathbb{1}. \quad (3.29)$$

The Werner state has concurrence equal to $(3p-1)/2$ and the maximal Bell factor is equal to $2p\sqrt{2}$. The Werner state is entangled for $p > 1/3$ and it is violating Bell inequalities for $p > 1/\sqrt{2}$

Amplitude damping channel

Quantum channel representing the dynamics of an atom spontaneously emitting a photon is known as an amplitude damping channel with Kraus operators being

$$A_0 = \begin{pmatrix} 1 & 0 \\ 0 & \sqrt{1-\gamma} \end{pmatrix}, \quad A_1 = \begin{pmatrix} 0 & \sqrt{\gamma} \\ 0 & 0 \end{pmatrix}. \quad (3.30)$$

When one qubit from the singlet is send via the amplitude damping channel the state at the output has the concurrence equal to $\sqrt{1-\gamma}$ and maximal Bell factor equal to $2\sqrt{2}(1-\gamma)$.

Phase damping channel

There is a quantum channel, phase damping channel, with exclusively quantum properties. The phase damping channel maintains the diagonal elements of the density matrix, therefore preserving the energy of quantum state but lowers the off-diagonal (phase) terms. It may describe a photon propagating via an optical fiber, where the phase of the photon is randomly perturbed by scattering. The Kraus operators of the phase damping are

$$A_0 = \begin{pmatrix} 1 & 0 \\ 0 & \sqrt{1-\gamma} \end{pmatrix}, \quad A_1 = \begin{pmatrix} 0 & 0 \\ 0 & \sqrt{\gamma} \end{pmatrix}. \quad (3.31)$$

When one qubit from then singlet is send via the amplitude damping channel the state at the output has the concurrence equal to $(1/2)(\sqrt{2-\gamma+2\sqrt{1-\gamma}} - \sqrt{2-\gamma-2\sqrt{1-\gamma}})$ and maximal Bell factor equal to $2\sqrt{1+(1-\gamma)^2}$

3.3 Quantum entanglement

Entanglement is the central notion we work with. Two chapters of the presented thesis deal with entanglement and entanglement recovery. The definition of quantum entanglement is usually done via notion of quantum separability. A composite quantum state ρ is separable if it can be expressed as a convex sum of its corresponding subsystems ρ_1, \dots, ρ_n :

$$\rho = \sum_i p_i \rho_1 \otimes \dots \otimes \rho_n \quad (3.32)$$

A state which is not separable is called entangled. The definition of an entangled state does not give us a straightforward direction to decide whether a particular state is entangled or not. Entanglement criteria providing this decision for various classes of quantum states were therefore introduced.

3.3.1 Entanglement of bipartite states

The entanglement between just two parties A and B is the simplest scenario we can study in this business. We are interested in correlations carrying by the quantum state ρ_{AB} shared by the two parties A and B .

Entanglement criteria

Very important entanglement criterion for bipartite states, called positive partial transpose (PPT), has been found by Asher Peres [69]. If ρ_{AB} is a separable state then a partially transposed matrix $\rho_{AB}^{T_B}$ is also a density matrix (has non-negative eigenvalues). In this thesis we deal mainly with bipartite states of two qubits and in such a case the PPT criterion is also a necessary condition of separability. In different words, system of two qubits is separable if and only if its partial transpose is a positive operator [70].

Another approach to characterize entangled states is via entanglement witnesses. The state ρ_{AB} is separable if it has a non-negative mean value $\text{Tr}(W\rho_{AB}) \geq 0$ for all observables W that (1) have non-negative mean value and (2) have non-negative mean on product states [70, 71].

LOCC and entanglement quantification

Since in this thesis we need to evaluate how much are our protocols successful, we have to quantify the amount of entanglement possessed by quantum state after our recovery stage. The initial idea for quantifying the entanglement is connected to the quantum teleportation protocol and the distillation of entanglement. In order to faithfully teleport a quantum state we need perfect (maximal) entanglement between the teleporting parties. However if the parties share just non-maximal entangled state the protocol would fail. The natural question is: Could we enhance the amount of entanglement just by an operation consisting from local operations performed by the two parties and classical communication between them? Yes, it is possible using the distillation protocol.

Distillation is able to prepare by local operations and classical communication (LOCC) a maximally entangled state from many copies of non-maximal entangled state. By LOCC procedure itself, without discarding or filtering some states, we could not increase the entanglement. So that rejecting some part of the ensemble is necessary part of the distillation protocol. Fact is that we cannot distill any entanglement from separable states, so that for distillation protocol to work at

least a bit of residual entanglement is needed. The supremum of rates by which we asymptotically approach the maximally entangled state Φ^+ is called *distillable entanglement*. It can be mathematically defined as follows

$$E_D(\rho) = \sup \left\{ r : \lim_{n \rightarrow \infty} \left(\inf_{\Lambda} \|\Lambda(\rho^{\otimes n}) - \Phi_{2^{rn}}^+\|_1 \right) = 0 \right\}, \quad (3.33)$$

where Λ is a LOCC operation, n number of copies of ρ . Such a defined quantification of entanglement is a protocol dependent. Distillable entanglement as a measure of entanglement only give sense for the task of distillation of quantum states. However to find the optimal distillation protocol is in general very complex task. For different task we would need different measure of entanglement suitable for that task.

Imagine we would like to reverse the process of distillation: create some state ρ from copies of maximally entangled state. A measure which arises from that task is called *entanglement of cost*.

$$E_C(\rho) = \inf \left\{ r : \lim_{n \rightarrow \infty} \left(\inf_{\Lambda} \|\rho^{\otimes n} - \Lambda(\Phi_{2^{rn}}^+)\|_1 \right) = 0 \right\}. \quad (3.34)$$

Pure bipartite states fulfill following equality $E_C = E_D$ but it does not hold generally for mixed states and multipartite states. In general there is an irreversibility between creation and distillation processes. As a consequence there exist so called bound entangled states which cannot be distilled. However Masanes in [72] showed that we can activate the bound entanglement so that it can be used for some non-classical task. In our discussions we only focus to an elementary unit of entanglement (ebit) represented by a two-qubit state, therefore the above complications are not present.

3.3.2 Bell inequalities

The entangled states carries correlations that has no classical counterpart. Such strong correlations were subject to discussion from the very beginning of the quantum theory. Einstein, Podolsky and Rosen (EPR) claimed according to their thought experiment [3] that quantum theory has to be incomplete because it cannot predict with certainty all the measurement results on the EPR pair (maximally entangled state). Bell showed in [4] that theories admitting criteria of EPR, now called local realistic theories, possess in state ρ maximal correlations given by inequality:

$$B = |\text{Tr}[\mathcal{B}\rho]| \leq 2, \quad (3.35)$$

where $\mathcal{B} = A_1 \otimes B_1 + A_1 \otimes B_2 + A_2 \otimes B_1 - A_2 \otimes B_2$ is a correlation operator. There are states in quantum theory that violate the Bell inequality (3.35). To say whether particular state violates Bell inequality we have to find a correlation operator (measurement) which is generally a nontrivial task.

For states consisting of two qubits the decision whether state ρ violates the Bell inequality is hidden in a property of so called correlation matrix t of the state ρ [73] emerging in expression (3.13). The elements of t are

$$t_{ij} = \text{Tr}(\rho \sigma_i \otimes \sigma_j). \quad (3.36)$$

The maximal violation of Bell inequality B_{max} (sometimes called maximal Bell factor) is then given by

$$B_{max} = \max B = 2\sqrt{t_{11}^2 + t_{22}^2}, \quad (3.37)$$

where t_{11} and t_{22} are two largest eigenvalues of the matrix $t^T t$. The B_{max} may be used as an entanglement measure for pure two-qubit states but not for mixed states because it is not entanglement monotone.

Every state that violates Bell inequality is entangled but the opposite implication is not true. There exist states that are entangled but does not violate the Bell inequality [74]. There has been shown [75] that B_{max} gives a fundamental limit on the prediction of measurement results in two complementary basis on the two-qubit state. It also represents a device independent detection of entanglement used in cases when the entire Hilbert space of the system is not precisely defined.

3.3.3 Entanglement measures

Another approach for quantifying entanglement uses axiomatically defined measures. Such measures can quantify entanglement independently on a given task.

Axioms of entanglement measure

There has to be given a list of possible postulates leading to plausible measures of entanglement (labeled as E). Plenio et. al. in [76] gave following list of axioms:

- *Monotonicity* axiom: Entanglement cannot increase under local operations

and classical communication.

$$E(\Lambda(\rho)) \leq E(\rho) \quad (3.38)$$

where $\Lambda(\rho) = \sum_i (A_i \otimes B_i) \rho (A_i^\dagger \otimes B_i^\dagger)$ is so called “separable operation”. Every LOCC operation can be written as a separable operation but not vice versa.

- *Separability* axiom: Entanglement vanishes on separable states.

$$E(\rho) = 0 \quad \text{if } \rho \text{ is separable} \quad (3.39)$$

Additional properties can be required from the entanglement measures, they are not necessarily needed for the consistency of the measure but in some context they are natural and suitable.

- The *normalization* condition assures suitable behaviour of entanglement measures. For the ensemble of n maximally entangled states $(\Phi_2^+)^{\otimes n}$ is

$$E((\Phi_2^+)^{\otimes n}) = n \quad (3.40)$$

- *Convexity* condition is often required:

$$E\left(\sum_i p_i \rho_i\right) \leq \sum_i p_i E(\rho_i) \quad (3.41)$$

- *Additivity* axiom. A measure satisfying

$$E(\rho^{\otimes n}) = nE(\rho) \quad (3.42)$$

is said to be additive.

- Some type of continuity condition may be required. The *asymptotic continuity* condition states the following:

$$\|\rho_n - \sigma_n\|_1 \rightarrow 0 \Rightarrow \frac{|E(\rho_n) - E(\sigma_n)|}{\log d_n} \rightarrow 0 \quad (3.43)$$

Examples of entanglement measures

I will briefly review most important measures of entanglement:

- *Relative entropy of entanglement*:

$$\inf_{\sigma \in \text{SEP}} \text{Tr} \rho (\log \rho - \log \sigma) \quad (3.44)$$

This measure is based on a distance of entangled state from the set of separable states.

- *Entanglement of formation* and following measures are based on “convex roof” approach. We first define an entanglement measure $E(\psi_i)$ on ensemble of pure states ψ_i only. Then we extend the measure to mixed states $\rho = \sum_i p_i |\psi_i\rangle\langle\psi_i|$ by convex roof operation:

$$E(\rho) = \inf \sum_i p_i E(\psi_i), \quad (3.45)$$

where the infimum is taken over all ensembles of $\{p_i, \psi_i\}$ satisfying $\rho = \sum_i p_i |\psi_i\rangle\langle\psi_i|$.

- *Schmidt number* is an extension of Schmidt rank from pure states to mixed states via convex roof:

$$r_S(\rho) = \min(\max_i [r_S(\psi_i)]) \quad (3.46)$$

- *Concurrence* C for two qubits in pure state was introduced by Wootters [77]

$$C = \langle \psi | \theta | \psi \rangle, \quad (3.47)$$

where θ is anti-unitary transformation $\theta\psi = \sigma_y \otimes \sigma_y \psi^*$. It can be straightforwardly extended to the mixed states: define an auxiliary matrix $\tilde{\rho}$ by $\tilde{\rho} = (\sigma_y \otimes \sigma_y) \rho^* (\sigma_y \otimes \sigma_y)$. The concurrence $C(\rho)$ of the qubit ρ is

$$C(\rho) = \max\{0, \lambda_1 - \lambda_2 - \lambda_3 - \lambda_4\}, \quad (3.48)$$

where the λ_i s are the square roots of the eigenvalues, in decreasing order, of the matrix $R = \rho \tilde{\rho}$.

- *Negativity* is a measure

$$N(\rho) = \frac{\|\rho^{T_2}\|_1 - 1}{2}, \quad (3.49)$$

where $\|A\|_1 = \text{Tr} \sqrt{A^\dagger A}$ is trace norm and ρ^{T_2} means partial transpose of ρ .

- Measure called *logarithmic negativity* is more often used than negativity

$$LN(\rho) = \log_2 \|\rho_{T_2}\|_1 \quad (3.50)$$

For other measures of entanglement follow the review [78].

The entanglement of formation can be expressed via concurrence with formula:

$$E(\rho) = H\left(\frac{1 + \sqrt{1 - C^2(\rho)}}{2}\right), \quad (3.51)$$

where H is entropy function $H(p) = -p \log p - (1 - p) \log(1 - p)$.

In chapters 4 and 5 we have introduced protocols which are able to recover in some cases a lost entanglement. To evaluate the quality of the solution we have used the concurrence as a measure of entanglement. The concurrence for two-qubit mixed states can be calculated by finding the eigenvalues of a specially designed matrix (3.48). The concurrences of the corresponding states during different stages of the localization protocol were calculated analytically. In quantum adaptation protocol we had to search for optimal solution using numerical methods, because we had to optimize the concurrence over all parameters of the recovery operations (quantum filtrations).

According to [79] we know that all entangled two-qubit states are distillable. Therefore we can use the distillable entanglement as a measure of entanglement for two-qubit states.

3.3.4 Entanglement of multipartite states

Entanglement of multipartite states has much more richer structure and its quantification is more complex task than in case of bipartite states. It involves different kind of correlation between the parties involved. The notion of separability is more branched compare to bipartite case. We can consider full multipartite separability via formula (3.32). But we can imagine also separability between group of parties with respect to some partition of the whole ensemble. Although in reality we always deal with multipartite states, physical situations in this thesis allow us to use models based on change of entanglement between two qubits.

3.4 Decoherence and evolution of entanglement

3.4.1 Decoherence

Quantum superposition postulate says that any coherent superposition of quantum states is also an allowed quantum state. Decoherence is a physical process that can destroy such a coherent superposition between states of a quantum system in a given preferred basis [24, 25].

We can distinguish three different types of physical mechanisms leading to decoherence.

Macroscopic fluctuations

Some parameters of a density matrix of the system may be influenced by macroscopic fluctuations. Then the off-diagonal elements of density matrix may be lowered and therefore cause the decoherence. There is no coupling with reservoir present (no entanglement). The fluctuations are rather slow and we could in principle undo its effect by sending a pulse probing the noise.

Generally we can express the dynamics of a density matrix ρ undergoing such a macroscopic fluctuations in the parameter ϕ of the evolution operator U by

$$\rho' = \int p(\phi)U(\phi)\rho U^\dagger(\phi)d\phi, \quad (3.52)$$

where we have performed an averaging over some probability distribution p and ρ' is an outgoing density matrix.

Imagine we have a polarization state of a photon which propagates via an optical fiber. The polarization state of the photon may be influenced by an effect called stochastic *polarization mode dispersion* (PMD). The fluctuation in birefringence changes the photon polarization randomly. Due to PMD the elements of the density matrix change along the propagation axis of the fiber. The off-diagonal elements of the density matrix exponentially decay and in infinite length (time) vanish.

Environment-induced selection

Decoherence process may be caused by coupling the system S with with some other quantum system A (let's call it apparatus), which creates an entangled state of the system - apparatus pair. In this point this model substantially differs from

the previous model of decoherence. When we trace out the apparatus degrees of freedom then the density matrix of the system turns into off-diagonal form. Such a view could on first sight solve the emergence of decoherence but it does not. The problem is the basis ambiguity of the apparatus states. Having two quantum systems only there is no reason for apparatus to monitor the system in e.g. a basis $\{|A_0\rangle, |A_1\rangle\}$, it could as well monitor in a different basis $\{|A_+\rangle, |A_-\rangle\}$. The question is: “What causes the preference of some states in the decoherence process?” Żurek shows that consistent theory of decoherence has to involve additional system called environment E , that interacts with the apparatus. The states of the apparatus are continuously monitored by the environment states and they effectively collapse to the preferred basis - pointer basis.

The simplest case of such a model of decoherence is given by a system consisting of three qubits, labeled by A , S , E to distinguish its role in the process. The process starts with a so called premeasurement where the system $|\psi\rangle = a|S_0\rangle + b|S_1\rangle$ is entangled with the apparatus :

$$(a|S_0\rangle + b|S_1\rangle)|A_0\rangle \rightarrow a|S_0\rangle|A_0\rangle + b|S_1\rangle|A_1\rangle \quad (3.53)$$

As we can see this state is basis ambiguous. Żurek solved this ambiguity by introducing system E that couples to the apparatus A

$$(a|S_0\rangle|A_0\rangle + b|S_1\rangle|A_1\rangle)|E_0\rangle \rightarrow |\phi\rangle = a|S_0\rangle|A_0\rangle|E_0\rangle + b|S_1\rangle|A_1\rangle|E_1\rangle \quad (3.54)$$

The environment consists usually from very large amount of systems. Explicit physical models show that the states of the environment become orthogonal asymptotically in time: $\langle E_0|E_1\rangle = 0$. The damping occurs on very short time scales so that in fact the decoherence is very rapid process even though the vanishing of off-diagonal terms appears asymptotically. We get the reduced state of the apparatus - system pair by tracing out the environment:

$$\rho_{AS} = \text{Tr}_E|\phi\rangle\langle\phi| = |a|^2|S_0\rangle\langle S_0|A_0\rangle\langle A_0| + |b|^2|S_1\rangle\langle S_1|A_1\rangle\langle A_1| \quad (3.55)$$

The joint state of system and apparatus is no more entangled and the state of the system

$$\rho_S = \text{Tr}_A[\rho_{AS}] = |a|^2|S_0\rangle\langle S_0| + |b|^2|S_1\rangle\langle S_1| \quad (3.56)$$

lost its coherence - decohered. The states of the apparatus are called pointer states.

Quantum erasing is a method for a full recovery of the coherence in the

system. The method turns the environmental degrees of freedom to a state where they lose the monitoring capacity on the system's degrees of freedom. The states of the system are forced to be again indistinguishable and coherence is recovered. Quantum erasing is in general very hard task because it has to control the whole complex environment.

Mixing distinguishable particles

The decoherence in both previous models behaved continuously in time. A discrete character of decoherence may be caused by incoherently mixing a system particle with some other particle, called “noise” particle. The particles are during the whole process in principal distinguishable. When we verify the coherence of the system particle our measurement apparatus is unable to distinguish between them (technical indistinguishability). The coherence of the system particle is lowered by a fixed amount coming from the presence of single “noise” particle only. Contrary to the above mentioned cases of decoherence this model behaves discretely. The decoherence changes in discrete steps proportional to the number of “noise” particles involved. The detailed study of this kind of decoherence is left to the chapter 6.

3.4.2 Evolution of entanglement

The decoherence process can affect not only superposition of quantum states but also the entanglement shared among parties. The quantum superposition generally decay asymptotically in time due to decoherence. We might therefore take as granted that the entanglement decay also asymptotically. That would mean that in every particular time the quantum state would possess a nonzero amount of entanglement and we could exploit distillation protocols to increase it.

Entanglement breaking channels

However the above statement is not true. There exist so called entanglement breaking channels that, no matter how strongly is the input state entangled always, produce non-entangled (separable) state. The entanglement breaking channel (EBC) Φ maps any quantum state to separable one. This is equivalent to the statement that state $(\mathbb{1} \otimes \Phi)|\beta\rangle\langle\beta|$ is separable for $|\beta\rangle = (1/\sqrt{d}) \sum_j |j\rangle \otimes |j\rangle$ a maximally entangled state in d-dimensions. The complete characterization of EBC was given in [80]. Qubit entanglement breaking channels were investigated

here [81].

Sudden death of entanglement

A weaker version of entanglement breaking property of quantum states were found by Yu and Eberly in [38]. They showed that in the preferred basis the entanglement of quantum state can in the presence of environment vanish in finite time. They have called the effect a Sudden Death of Entanglement (SDE). The SDE is in general dependent on input states and we may sometimes avoid its effect by simply using different input states carrying the same amount of entanglement as the initial states.

3.5 Numerical methods

The complexity of the adaptation of quantum channels presented in this thesis demanded the usage of modern techniques of numerical analysis. We have used novel global optimization methods to search for global maximum. They are based on new genetic and migration algorithms giving better results than conventional local search algorithms.

Global optimization is a procedure (algorithm) that searches for optimal parameters which give extremal value of a function, called an objective function. The objective function is a mapping $f : X \mapsto \mathbb{R}$, where the domain X can contain any given type of elements. It is not necessary that the objective function is a function with definite prescription, it can also be a result of numerical calculation (algorithm).

The global optimization techniques are very complex in general. The objective function can have multiple local extrema and global extrema. The important part of the global optimization algorithm is a decision where to search in next step of the algorithm, so called *heuristic*. By proper heuristic we can minimize the chance to get stuck in local minimum. The global optimization business started its grow after first computers were available in the second half of the twentieth century. Basically two classes of global optimization algorithms can be distinguished: deterministic and probabilistic (stochastic) ones.

Deterministic algorithms can be simulated by a deterministic finite automaton. It is a device that consists of an input alphabet, set of states, initial state, set of final states and transition function which with the knowledge of current state of the automaton and an input word from alphabet, produces the next state the

automaton will be in. Deterministic algorithms are mostly based on “divide and conquer” principle. Roughly, the “divide and conquer” methods exploits division of the search space into smaller pieces where we look for an optimal solution, the results are collected and then all the solutions over all pieces are compared and the best among them is chosen.

Probabilistic (stochastic) global optimization can be simulated also by the finite automaton but with probabilistic stochastic transition function. There has to be a source of random events which is used for decision about the next state of the automaton. The presence of random element in the procedure may cause failure to find the optima in finite amount of computation, therefore instead of heuristic a term *metaheuristic* is used. However the global stochastic algorithms can usually more efficiently escape from the local optima and search in different part of space than the deterministic algorithms.

Large class of probabilistic global optimization algorithms is based on evolution principle taken from Nature. The evolution algorithm uses metaheuristic inspired by biological mechanisms of inheritance, mutation, crossover, natural selection and survival of the fittest. A genetic algorithm (GA) is one class of many evolution algorithms we know today. It was developed by John Holland in 1970's. GA is best suited for problems when the objective function is discontinuous, non-linear, stochastic, has unreliable or undefined derivatives. In the chapter 4 about adaptation of quantum channels a search for global optima of concurrence over filtrations operations has to be performed. There is used biological terminology in GA business. The basic genetic algorithm is based on following steps written symbolically in pseudo code:

```
{
  Initialize population;
  Evaluate population;

  while Termination_Criteria_Not_Satisfied

  {
    Selection of parents for reproduction;
    Perform crossover;
    Perform mutation;
    Accept new generation;
    Evaluate population;
  }
```


}

Initially we have to choose proper representation of the state space of chromosomes and create random population of chromosomes. We have to evaluate the fitness of each chromosome in the population. Then we enter the loop and repeat following steps until we fulfill the termination criteria: Selection step chooses a list of parents for reproduction. It ensures that parents with better fitness have better chances to produce offspring. Crossover is used to create a child by combining the features of two parents. Mutation creates child by modifying with some probability the parent genes.

Later in time we have found another algorithm called “Self organizing migration algorithm” (SOMA) based also on evolution idea. SOMA is migration algorithm (MA) motivated by social behaviour of some mammals (e.g. wolfs searching for food). SOMA works on population of candidate solutions in loops, called migration loops. The population is initialized randomly over the search space. In each loop the fitness of the whole population is evaluated and a individual with highest fitness becomes a leader. In one migration loop all individuals will move in the direction of the leader. The path of the migration is randomly chosen. The movement of an individual from position \vec{r}_0 to a new position \vec{r} can be given by a formula

$$\vec{r} = \vec{r}_0 + tm\vec{P}, \quad (3.57)$$

where $t \in [0, \text{path length}]$, m is a difference between the leader and start position of a individual, \vec{P} control vector for movement perturbation. The vector \vec{P} causes an individual to move toward the leading individual.

We have used the free implementation of GA to MATLAB environment called Genetic Algorithm Optimization Toolbox available here [82]. The source codes of SOMA (self-organizing migration algorithm) are available free for MATLAB, Mathematica, C language and others here [83]. We have adopted the above mentioned programs to suit our needs and created set of programs based on them that searched for global maximum and also provided the necessary self-check. We have found the utility very successful in searching. In some cases it gave us also a generic answer to the problem.

3.6 Experimental methods and techniques

We have proposed proof of principle experiments in chapters 5 resp. 6 to test the theoretical predictions.

The experiment described in chapter 5 was performed in the group of Prof De Martini at the Dept of Physics, University of Rome, Italy by the experimentalists Fabio Sciarrino, Eleonora Nagali and Francesco de Martini. The other experiment described in chapter 6 was performed at Palacky University in Olomouc, the Czech Republic by experimentalist Lucie Čelechovská, Jan Soubusta and Miloslav Dušek.

The details of the particular experiments are provided in the corresponding chapters.

Part II
Research Work

Chapter 4

Adaptation of Quantum Channels

In this chapter, a probabilistic quantum filtering is proposed to properly adapt sequential independent quantum channels in order to stop sudden death of entanglement. In the adaptation, the quantum filtering does not distill or purify more entanglement, it rather properly prepares entangled state to the subsequent quantum channel. For example, the quantum adaptation probabilistically eliminates the sudden death of entanglement of two-qubit entangled state with isotropic noise injected into separate amplitude damping channels. The result has a potential application in quantum key distribution through noisy channels.

4.1 Introduction

Recently, it has been recognized that the entanglement can be totally lost if a noisy entangled state is inserted into a channel which is entanglement preserving for all the channel parameters (such as the amplitude and phase damping channel) [38, 84, 85, 46]. Such the behavior is called the sudden death of entanglement (SDE). It is interesting how to stop the SDE, deterministically or even probabilistically, at a cost of success rate of the transmission of entanglement.

The SDE has been reported as a property of a given non-maximally entangled state passing through the quantum channel representing a finite-time continuous interaction with a reservoir. A state preparation of the non-maximally entangled state is considered to be independent from the subsequent noisy channel. Let us to describe this situation in more abstract way. Such the non-maximally entangled state can be generally understand as an output from some previous independent channel applied on this maximally entangled state. Thus we have a composite of two independent channels. The reservoirs corresponding to these two channels are therefore considered to be independent. It very well corresponds to a broad

class of realistic physical situations in which the reservoirs of two channels are not interacting. Optimizing over input represented by maximally entangled states it can be recognized whether the composite channel, exhibiting SDE, is actually entanglement breaking channel [81]. For the entanglement breaking channel, no entanglement propagates through the channel. Also no entanglement can be distilled after the channel. Below, the SDE will be understood rather as a property of a composition of channels with independent reservoirs. It is not always possible to split a given quantum channel into independent sub-channels. Then the reservoirs corresponding to sub-channels are not independent and their exact dynamics and coupling have to be studied in a detail. We will focus just on the case of independent channels.

We study two-qubit entanglement undergoing local unitary quantum dynamics. This means that each qubit interacts just with its own reservoir resulting in channels for which the Kraus decomposition is valid [86]. We concern only about the cases when the SDE in the composite channel breaks entanglement completely. To stop the SDE, single-copy distillation [63, 87, 88, 89] can be sometimes simply placed between the channels. Then distillation increases entanglement before the subsequent channel and any construction of the distillation is only optimized with a respect to the state after the previous channel.

We propose an adaptation of quantum channels to prevent the SDE. The probabilistic adaptation differs from the single-copy entanglement distillation and purification [63, 87, 88, 89]. In the adaptation, even in the case that the entanglement could not be increased by single-copy distillation after first channel, still the entangled state can be better prepared to the subsequent channel to preserve entanglement. Basically, the proper adaptation depends on the subsequent noisy channel. As will be demonstrated, it can help to stop the SDE when the single-copy distillation is inefficient. It is rather complex problem to find generally optimal adaptation between the channels. Therefore we rather discuss realistic examples of the SDE to demonstrate a potential power of the adaptation. First, we concentrate on a simple example of two subsequent single-qubit non-unital channels with an anisotropic noise. We show by optimal unitary adaptation of such the channels, the SDE is completely canceled for all the channel parameters. Second, probabilistic adaptation between the channel with an isotropic noise and the subsequent amplitude damping channel is analyzed. In this case, the SDE cannot be stopped by the unitary adaptation. But if the probabilistic adaptation is applied then the SDE vanishes completely. It demonstrates, that the SDE can be partially or even fully caused by the improper adaptation of the noisy channels. To find whether the SDE is really presented, it is necessary to discuss

the optimal adaptation and then analyze if the entanglement passing through the adapted channels will be broken or not. Such the results have a direct application in quantum key distribution through composite realistic channels and in a multi-qubit version, also in the cluster-state preparation for quantum computing.

4.2 Quantum Adaptation of Independent channels

From our point of view, the SDE is an entanglement breaking property of a composition of independent quantum channels if at least single one is not entanglement breaking at all. We assume any particle from entangled state evolves locally unitarily and reacts just with its own reservoir. Reservoirs are mutually independent. For such a case we may describe the evolution of the entangled state by using independent quantum channels in the form of Kraus decomposition [90]

$$\chi(\rho) = \sum_{i=1}^N A_i \rho A_i^\dagger, \quad (4.1)$$

where $\sum_k A_k^\dagger A_k = \mathbb{1}$. An important class of the channels are unital channels (for example, depolarization channel or phase damping channel), which preserves the isotropic noise. Such the channels transform maximal entangled state only to a mixture of maximally entangled states. The channel is entanglement breaking if no entanglement remains although any maximally entangled state $|\Psi\rangle_{AB}$ is passing through the channel [81]. Mathematically, for single-qubit channel it corresponds to a condition based on positive partial transposition criterion [73, 69], explicitly $[\chi_B(\rho_{AB})]^{TA} \geq 0$, where $\rho_{AB} = |\Psi\rangle_{AB}\langle\Psi|$. After such the channel no entanglement can be distilled even by multi-copy distillation [65, 67, 79].

The basic asymmetrical and symmetrical configurations of the propagation of two-qubit maximally entangled state through independent noisy channels are depicted on Fig. 4.1. In the first case, a single qubit from maximally entangled two-qubit state $\rho_{AB} = |\Psi\rangle_{AB}\langle\Psi|$ is propagating through two independent channels χ_{B1} and χ_{B2} having mutually independent reservoirs. In the second case, both the qubits are symmetrically propagating through independent (but simply identical) consecutive channels χ_{A1}, χ_{A2} and χ_{B1}, χ_{B2} all having mutually independent reservoirs. The maximally entangled state ρ_{AB} passing through the

asymmetrical composition of two channels $\chi_{B2} \circ \chi_{B1}(\rho_{AB})$ can be described as

$$\chi_{B2} \circ \chi_{B1}(\rho_{AB}) = \sum_{i=1}^{N_1} \sum_{j=1}^{N_2} B_{2j} B_{1i} \rho_{AB} B_{1i}^\dagger B_{2j}^\dagger \quad (4.2)$$

and the composite channel is entanglement breaking if

$$[\chi_{B2} \circ \chi_{B1}(\rho_{AB})]^{T_A} \geq 0. \quad (4.3)$$

For the symmetrical configuration, the maximally entangled state going through the symmetrical both-side channels is transformed to

$$\chi_{A2} \circ \chi_{A1} \circ \chi_{B2} \circ \chi_{B1}(\rho_{AB}) = \sum_{i,k=1}^{N_1} \sum_{j,l=1}^{N_2} B_{2i} B_{1j} A_{2k} A_{1l} \rho_{AB} A_{1l}^\dagger A_{2k}^\dagger B_{1j}^\dagger B_{2i}^\dagger \quad (4.4)$$

and the composite channel is entanglement breaking if

$$[\chi_{A2} \circ \chi_{A1} \chi_{B2} \circ \chi_{B1}(\rho_{AB})]^{T_A} \geq 0. \quad (4.5)$$

For the asymmetrical situation, the entanglement breaking property does not depend on a kind of maximally entangled state [81], but for the symmetrical configuration it is not generally true [85]. The channel is sequentially entanglement preserving if

$$[\chi_{B_i}(\rho_{AB})]^{T_A} < 0, \quad [\chi_{A_i}(\rho_{AB})]^{T_A} < 0 \quad (4.6)$$

and only such the channels will be taken into consideration. If the channel is not sequentially entanglement preserving then the entanglement cannot be successfully transmitted with a help of any adaptation method. Also the composite channels preserving entanglement will be simply omitted in the following discussion. It is obvious that two consecutive channels can break entanglement although they do not break it separately. But this is not non-trivial effect of the SDE. A non-trivial feature of the SDE [38, 84, 85, 46] is that each channel is entanglement preserving separately but the whole concatenation (whole channel) is entanglement breaking. Physically, we have different independent channels preserving entanglement for any value of finite channel parameters. But their combination exhibiting the SDE can give entanglement breaking channel for some values of channels parameters. Since it is impossible to improve the composite channel just by the operations before and after the channel, it is non-trivial case of the SDE.

To stop the SDE in the composite channel, a single-copy quantum filter can be generally placed between the individual channels. The quantum filter on

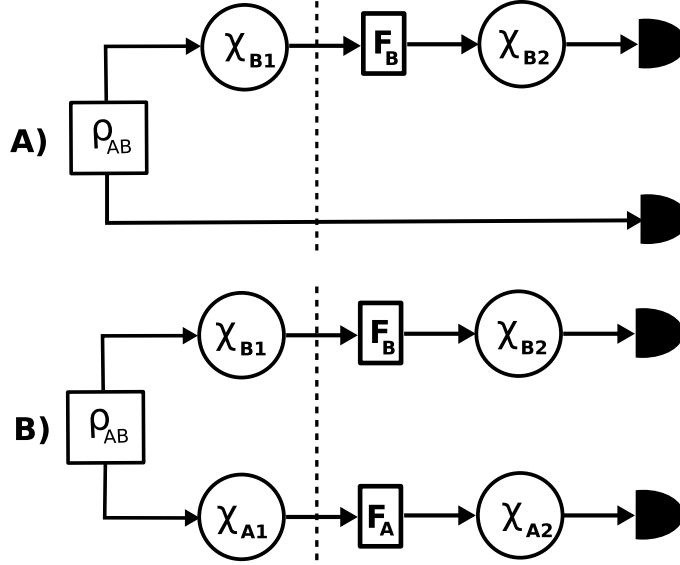


Figure 4.1: The channel adaptation for the maximally entangled state passing through asymmetrical (A) and symmetrical (B) pairs of the independent channels with local unitary dynamics, dashed lines part the protocol virtually to the preparation stage (mixed state from maximally entangled state) (left) and to the other stages (right): ρ_{AB} – maximally entangled state, $\chi_{Ai,Bi}$ – quantum channels, $F_{A,B}$ – quantum filters.

single-qubit state can be described by the transformation

$$\rho' = \frac{F\rho F^\dagger}{\text{Tr}(F\rho F^\dagger)}, \quad (4.7)$$

where $F^\dagger F \leq \mathbb{1}$. Generally, the quantum filtering can be decomposed as $F = UF_0V$, where U, V are single-qubit unitary operations and $F_0 = \text{diag}(1, \sqrt{r})$, $0 \leq r \leq 1$. If $r = 1$ the filtering is reduced just to unitary operation. It was theoretically described that such the local filtration applied after the noisy channel can increase entanglement [63, 87, 88]. Recently, the local filtering has been experimentally demonstrated for entangled pair of photons generated from spontaneous parametric down-conversion [89]. The result of the optimal local filtration always approaches the mixture of Bell diagonal states, from which more entanglement cannot be further distilled by any single-copy local filters. It automatically excludes a chance to stop the SDE for a composition of the unital channels. On the other hand, for the non-unital channels the single copy filtration could be able to increase entanglement or perform proper adaptation of the channels.

With the filters between the channels, after the asymmetrical channels in the

configuration (A) the maximally entangled state is

$$\chi_{B2} \circ F_B \circ \chi_{B1}(\rho_{AB}) = \frac{1}{S} \sum_{i=1}^{N_1} \sum_{j=1}^{N_2} B_{2j} F_B B_{1i} \rho_{AB} B_{1i}^\dagger F_B^\dagger B_{2j}^\dagger, \quad (4.8)$$

where the success rate is $S = \sum_{i=1}^{N_1} \text{Tr}(F B_{1i} \rho_{AB} B_{1i}^\dagger F^\dagger)$. On the other hand, the composition symmetrical channels (B) with the inter-mediate filtration produces

$$\begin{aligned} & \chi_{A2} \circ F_A \circ \chi_{A1} \circ \chi_{B2} \circ F_B \circ \chi_{B1}(\rho_{AB}) = \\ & \frac{1}{S} \sum_{i,k=1}^{N_1} \sum_{j,l=1}^{N_2} B_{2i} F_B B_{1j} A_{2k} F_A A_{1l} \rho_{AB} A_{1l}^\dagger F_A^\dagger A_{2k}^\dagger B_{1j}^\dagger F_B^\dagger B_{2i}^\dagger, \end{aligned} \quad (4.9)$$

where the success rate is

$$S = \sum_{j,l=1}^{N_2} \text{Tr}(F_A A_{1l} F_B B_{1j} \rho_{AB} B_{1j}^\dagger F_B^\dagger A_{1l}^\dagger F_A^\dagger). \quad (4.10)$$

The task considered here is, by the application of quantum filters, transmit the entanglement through the composite channel which is entanglement breaking. It means to find if the composite channel, satisfying (4.3,4.6) or (4.5,4.6), will preserve entanglement, i.e. will fulfill the conditions

$$[\chi_{B2} \circ F_B \circ \chi_{B1}(\rho_{AB})]^{T_A} < 0 \quad (4.11)$$

or

$$[\chi_{A2} \circ F_A \circ \chi_{A1} \circ \chi_{B2} \circ F_B \circ \chi_{B1}(\rho_{AB})]^{T_A} < 0 \quad (4.12)$$

at a cost of success rate of the filtration. It is impossible to solve such the complex task analytically for all the compositions of any channels, even for some specific channels it is sophisticated. Therefore, rather than general answer we will analyze some physically interesting examples (for example, previously published in Ref. [85]) to demonstrate that adaptation by single-copy filtration or even just unitary operation can be powerful tool to stop the SDE.

4.3 Asymmetrical example

The simplest example of the adaptation for the asymmetrical configuration (A) is following. In the asymmetrical configuration, the channel χ_{B1} (χ_{B2}) transmits any qubit state either perfectly with a probability p_1 (p_2) or, with probability $1 - p_1$

$(1 - p_2)$, the qubit is completely lost and another qubit in the pure state $|0\rangle$ ($|1\rangle$) occurs in the channel. Here, for simplicity, we use just two orthogonal states but similar analysis can be done for two general mixed states. It is easily to check that both the channels are entanglement preserving for $p_1, p_2 > 0$. If such the channels are combined, the maximally entangled state $|\Psi_-\rangle = (|01\rangle - |10\rangle)/\sqrt{2}$ is transformed to the mixture

$$\rho = p_1 p_2 |\Psi_-\rangle \langle \Psi_-| + \frac{p_2(1-p_1)}{2} \mathbb{1} \otimes |0\rangle \langle 0| + \frac{1-p_2}{2} \mathbb{1} \otimes |1\rangle \langle 1|, \quad (4.13)$$

which is entangled (using partial transposition criterion [73, 69]) if and only if $p_1, p_2 \neq 0$ satisfy

$$p_2 > \frac{1-p_1}{1-p_1+p_1^2}. \quad (4.14)$$

Then outgoing two-qubit state has the concurrence [77]

$$C(\rho) = p_1 p_2 - \sqrt{(1-p_1)(1-p_2)p_2}. \quad (4.15)$$

Otherwise the composite of these two channels is entanglement breaking. This is the SDE apparently accompanied by the entanglement breaking. But fortunately, if the unitary transformation making $|0\rangle \leftrightarrow |1\rangle$ is simply applied between the channels, then the density matrix changes to

$$\rho' = p_1 p_2 |\Phi_-\rangle \langle \Phi_-| + \frac{1-p_1 p_2}{2} \mathbb{1} \otimes |1\rangle \langle 1|, \quad (4.16)$$

where $|\Phi_-\rangle = (|00\rangle - |11\rangle)/\sqrt{2}$, which is always entangled for any $p_1, p_2 \neq 0$. All the entanglement breaking channels vanish just simply by the unitary operation. If two general states are considered instead of $|0\rangle$ and $|1\rangle$, the unitary transformation depends on both the channels. The same result can be obtained for any maximally entangled state entering into the channels. The amount of entanglement is simply given by the concurrence $C'(\rho) = p_1 p_2$. As a result, practically, the composite channel is not entanglement breaking channel at all (for $p_1 p_2 > 0$). The entanglement can be further enhanced using local filtering after the composite channel to approach maximal concurrence $C''(\rho) = \sqrt{p_1 p_2}$. The optimal filtering is $|11\rangle \rightarrow \sqrt{p_1 p_2} |11\rangle$ and $|01\rangle \rightarrow \epsilon |01\rangle$, where $\epsilon \rightarrow 0$. It is evidently a simple witness that even unitary adaptation between the different channels can stop the SDE.

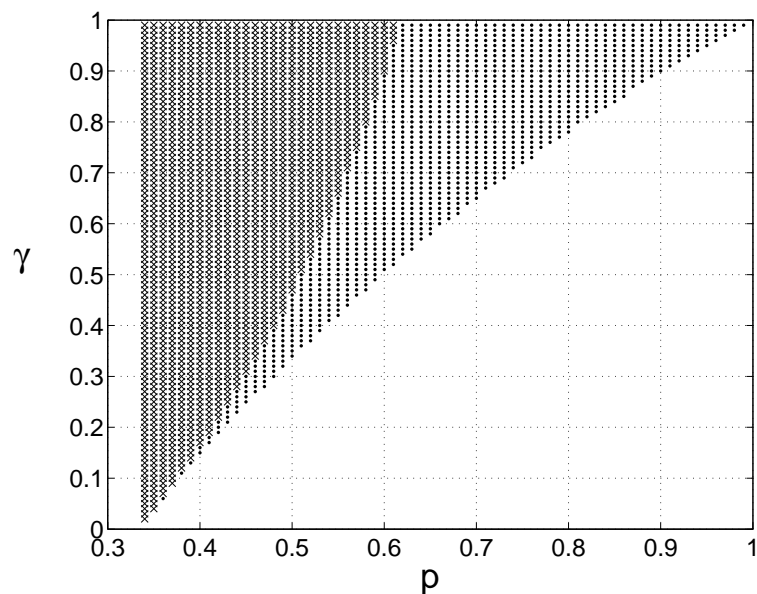


Figure 4.2: The quantum adaptation for the maximally entangled state passing through symmetrical pairs of consecutive depolarizing and amplitude damping channels. Numerical optimization has been performed in a net of the points. SDE happens for input $|\Phi_{-}\rangle$ in the union of crosses and dots and for input $|\Psi_{-}\rangle$ just in the area of crosses. The entanglement breaking happens just in the area of crosses due to possible unitary conversion between input states. The entanglement breaking in the area of crosses can be undone by our quantum adaptation procedure. In the area where $p < 1/3$, the entanglement is broken already in the depolarizing channel, on the other hand, the white area on the right is not interesting since the entanglement is preserving.

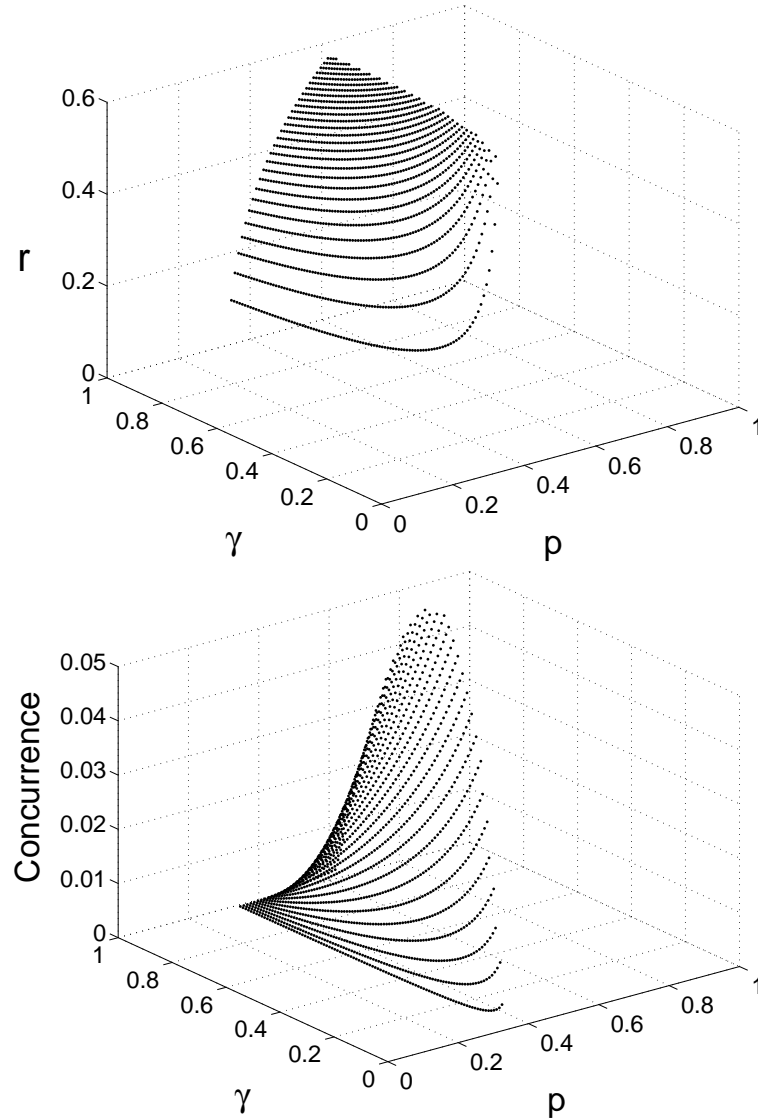


Figure 4.3: The plot of optimal parameter r of a diagonal filter depending on the parameters γ and p of the channels (top figure) and the plot of concurrence depending on the parameters γ and p of the channels (bottom figure). Both plots are results of the quantum adaptation for the sequence of depolarizing and amplitude damping channel. We used diagonal filters $F_A, F_B = \text{diag}(1, \sqrt{r})$ for the adaptation.

4.4 Symmetrical example

In the following example, we show that the SDE can depend on the input maximally entangled state in the symmetrical configuration and the adaptation by the unitary operation is then insufficient to reduce the break of entanglement. But using quantum filters, the break of entanglement can be completely eliminated. Remind, if the filter is placed between the channels to improve the transmission, it can just increase the entanglement from the first channel at the maximum and then it can be send through the second channel. But such the cases cannot be understand as the adaptation, it is exactly the known single-copy distillation [63, 87, 88]. The adaptation means that the filter depends also on the parameters of the subsequent channel. Since the filtering cannot increase the entanglement of the mixture of the Bell states, the states with isotropic noise [74]

$$\begin{aligned}\rho'_1 &= p|\Psi_-\rangle\langle\Psi_-| + \frac{1-p}{4}\mathbb{1} \otimes \mathbb{1}, \\ \rho'_2 &= p|\Phi_-\rangle\langle\Phi_-| + \frac{1-p}{4}\mathbb{1} \otimes \mathbb{1},\end{aligned}\quad (4.17)$$

where $|\Phi_-\rangle = (|00\rangle - |11\rangle)/\sqrt{2}$, after the first channels are good candidates to see an effect of the adaptation. For both the states, the entanglement is preserved if $p > 1/3$. The states (4.17) can outcome from the depolarizing channel acting on single (or both) of the qubits. The depolarizing channel on single qubit is represented by the set of the Kraus operators

$$D_3 = \sqrt{\frac{1+3p}{4}}\mathbb{1}, \quad D_i = \sqrt{\frac{1-p}{4}}\sigma_i \quad (4.18)$$

where $i = 1, 2, 3$ and σ_i are the Pauli matrices

$$\sigma_1 = \begin{pmatrix} 0 & 1 \\ 1 & 0 \end{pmatrix}, \quad \sigma_2 = \begin{pmatrix} 0 & -i \\ i & 0 \end{pmatrix}, \quad \sigma_3 = \begin{pmatrix} 1 & 0 \\ 0 & -1 \end{pmatrix}. \quad (4.19)$$

The depolarization is common physical decoherence process, it can arise from the random isotropic unitary changes of the state in the channel.

Such the states (4.17) are then locally processed by the filters F_A, F_B and then entry into the identical amplitude damping channels acting symmetrically on both the qubits. The amplitude damping channel is non-unital channel described by the Kraus matrices

$$A_1 = \begin{pmatrix} 1 & 0 \\ 0 & \sqrt{1-\gamma} \end{pmatrix}, \quad A_2 = \begin{pmatrix} 0 & \sqrt{\gamma} \\ 0 & 0 \end{pmatrix}. \quad (4.20)$$

It often arises from a resonant interaction of qubit system with zero-temperature reservoir characterized by a Hamiltonian $H_A = \sum_k g_k \sigma_- a_k^\dagger + g_k^* \sigma_+ a_k$, where $\sigma_\pm = \frac{1}{2}(\sigma_1 \pm i\sigma_2)$ are operators of the two-level system, a_k, a_k^\dagger are the reservoir operators, g_k is coupling constant and the averaging is over the modes of reservoir, for review [91]. Physically, the source of decoherence is then just the spontaneous emission of the two-level system. This non-unital amplitude damping channel will not break the entanglement for any $\gamma \in (0, 1)$, corresponding to finite time dynamics. This channel has been used in Ref. [85], where non-trivial SDE has been recognized.

For the symmetrical configuration, the SDE depends on the input maximally entangled state. In the Fig. 4.2 for channel parameters in the union of crosses and dots the SDE occurs for the input state $|\Phi_-\rangle$ whereas for the input state $|\Psi_-\rangle$ SDE appears just in the area of crosses. The unitary adaptation is able to make conversion between these cases without any reduction of the break of entanglement. But the same effect can be obtained if the input maximally entangled state is changed. Therefore, in the region of dots the SDE is not accompanied by the break of entanglement. Thus unitary adaptation cannot help to stop the break of entanglement at all, contrary to the previous example.

Interestingly, quantum filtering can help to adapt the channels each to other. Even for this specific example, it is complex to find the optimal filter analytically. From this reason, the numerical genetic and SOMA algorithms for function optimization have been used [82, 83]. The optimization has been performed in a net of the points and at the end, the optimized filters have been used to check their ability to stop the SDE. There has been included, beside quantum filters, also unitary operations into the optimization routine. The results of numerical calculations are depicted in Fig. 4.2. In all the numerically analyzed cases, the SDE is corrected (denoted by crosses). From the numerical optimization, it is also possible to find that a quantum filtering is sufficient even taking both the filters in the basis of the amplitude damping and identical thus $F_A, F_B = \text{diag}(1, \sqrt{r})$ can be simply used. From the partial transposition criterion [73, 69], it is possible to derive a sufficient condition

$$0 < \sqrt{r} < \frac{2\sqrt{p(1+p)} - (1+p)}{\gamma(1-p)} \quad (4.21)$$

for the quantum filters to stop the break of entanglement. The success rate of the filtration is then $S = p(1 - \sqrt{r})^2 + (1 + \sqrt{r})^2$. To find optimal filter and the concurrence after the adaptation, the numerical optimization still has to be performed. The results are depicted on Fig. 4.3, where the optimal parameter r of the filter and maximal value of the concurrence are plotted as functions of the

channel parameters γ and p . Evidently, in all the cases, the filtering completely eliminates the SDE caused by the symmetrical amplitude-damping channels.

4.5 Conclusion

We have proposed and investigated an adaptation protocol for quantum channels that can adapt concatenation of two quantum channels that is as a whole entanglement breaking. Each of the channels is entanglement preserving but together they are entanglement breaking so that we cannot use distillation protocols acting just before or behind the whole channel. We can also imagine that a preparation of a mixed entangled state entering the second channel is a result of sending a maximally entangled state to the first channel. The two-channel model thus describes a very broad class of entanglement breaking situations. The protocol in general exploits quantum filtrations operating between the channels. The adaptation protocol is thus dependent on parameters of both the preceding and the following channel and substantially differs from the distillation protocol.

Two different scenarios were investigated an asymmetrical and symmetrical one. For the asymmetrical configuration we used a quantum channel that with some probability lets the input state intact and with the rest probability confuses the input state with different state. We have shown that a concatenation of two channels of the above kind and being entanglement breaking, may be turned back to entanglement preserving just by using unitary transform between the channels. In the symmetrical configuration we showed that a concatenation of pairs of depolarizing and amplitude damping channels has for some channel parameters the entanglement breaking property. The entanglement breaking can be fully undone in this example by proper quantum filtrations applied between the pairs of subsequent channels.

The results of our investigation were published here:

- **M. Gavenda and R. Filip**, *Quantum adaptation of noisy channels*, Phys. Rev. A **78**, 052322 (2008).

Chapter 5

Entanglement localization

We discuss, in this chapter, both theoretically and experimentally elementary two-photon polarization entanglement localization after break of entanglement caused by linear coupling of environmental photon with one of the system photons. The localization of entanglement is based on simple polarization measurement of the surrounding photon after the coupling. We demonstrate that non-zero entanglement can be localized back irrespectively to the distinguishability of coupled photons. Further, it can be increased by local single-copy polarization filters up to an amount violating Bell inequalities. The present technique allows to restore entanglement in that cases, when the entanglement distillation does not produce any entanglement out of the coupling.

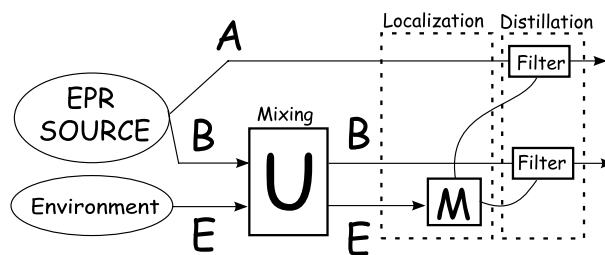


Figure 5.1:

5.1 Introduction

Quantum entanglement, the fundamental resource in quantum information science, is extremely sensitive to coupling to surrounding systems. By this coupling the entanglement is reduced or even completely vanishes. In the case of partial entanglement reduction, quantum purification and distillation protocols can be adopted [66, 67, 92, 49, 93]. In quantum distillation protocols, entanglement can be increased without any operation on the surrounding systems. Using a collec-

tive procedure, the distillation probabilistically transforms many copies of less entangled states to a single more entangled state, using a collective procedure just at the output of the coupling [48]. Fundamentally, the distillation requires at least a bit of residual entanglement passing through the coupling.

When the coupling with the environment completely destroys the entanglement, both purification and distillation protocols can not be exploited. Hence another branch of methods like unlocking of hidden entanglement [54] or entanglement localization [94, 95, 96, 60, 97] must be used. In reference [54] there has been estimated that in order to unlock the hidden entanglement from a separable mixed state of two subsystems an additional bit or bits of classical information is needed to determine which entangled state is actually present in the mixture. However no strategy was presented in order to extract this information from the system of interest or the environment. Latter, to retrieve the entanglement, the localization protocols [94, 95, 96, 60, 97] have been introduced working on the principle of getting some nonzero amount of bipartite entanglement from some multipartite entanglement. That means performing some kind of operation on the multipartite system (or on its part) may induce bipartite entanglement between subsystems of interest.

We can say that the entanglement breaks because it is so inconveniently redistributed among system of interest and environment that it is transformed into generally complex multipartite entanglement. Entanglement can be localized back for the further application just by performing suitable measurement on the surrounding system and the proper feed-forward quantum correction see Fig. 5.1. The measurement and feed-forward operation substitute, at least partially, a full inversion of the coupling which requires to keep very precise interference with the surrounding systems. For many-particle systems, the maximal value of the localizable entanglement depends on the coupling and also on initial states of surrounding systems.

To understand the mechanism of the entanglement localization, we simplify the complex many particle coupling process to a set of sequential couplings with a single particle representing an elementary surrounding system E [24]: see FIG. 5.2. Then, our focus is just on the three-qubit entanglement produced by this elementary coupling of one qubit from maximally entangled state of two qubits A and B to a third surrounding qubit E . Before the coupling to the qubit B , we have typically no control on the quantum state of qubit E , hence considered to be unknown. Further, the qubit E is typically not interfering or weakly interfering with the qubit B .

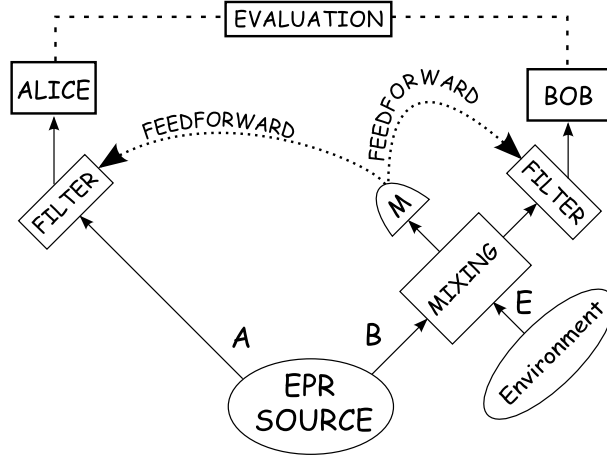


Figure 5.2:

5.2 Theory

Let us assume that we generate a maximally entangled polarization state $|\Psi_{-}\rangle_{AB} = (|HV\rangle - |VH\rangle)/\sqrt{2}$ of two photons A and B . The form of the maximally entangled state is not relevant, as the same results can be obtained for any maximally entangled state. The first photon is kept by Alice and second is coupled to the surrounding photon E in an unknown state, $\rho_E = \mathbb{1}/2$ (completely unpolarized state), by a simple linear polarization insensitive coupling (a beam splitter with transmissivity T). After the coupling, three possible situations can be observed: both photons B and E go simultaneously to either mode k'_B or mode k'_E , or only a single photon is separately presented in both output modes k'_B or k'_E (see FIG. 5.2). We will focus only on the last case, that is a single photon output from the coupling. In this case, it is in principle not possible to distinguish whether the output photon is the one from the entangled pair (B) or the unpolarized photon E . We investigate in detail, the impact of the coherence of the surrounding system on the localization procedure. Note that the system E can be also produced by the entanglement source and then coupled to the entangled state through a subsequent propagation. Therefore, it is not fundamentally important whether E is produced by truly independent source or not.

5.2.1 Coherent coupling

To understand the role of partial coherence in the entanglement localization, let us first assume that both photons B and E are perfectly coherent (in principle indistinguishable). Then, if both the photons leave the linear polarization-insensitive coupling separately, the coupling transformation can be written for

any polarization state $|\Psi\rangle_B$ as:

$$\begin{aligned} |\Psi\rangle_B|\Psi\rangle_E &\rightarrow (T-R)|\Psi\rangle_B|\Psi\rangle_E, \\ |\Psi\rangle_B|\Psi_\perp\rangle_E &\rightarrow T|\Psi\rangle_B|\Psi_\perp\rangle_E - R|\Psi_\perp\rangle_B|\Psi\rangle_E. \end{aligned} \quad (5.1)$$

Both the singlet state $|\Psi_-\rangle_{AB}$ as well as ρ_E can be written in the general basis $|\Psi\rangle$ and $|\Psi_\perp\rangle$, namely: $|\Psi_-\rangle_{AB} = (|\Psi\Psi_\perp\rangle_{AB} - |\Psi_\perp\Psi\rangle_{AB})/\sqrt{2}$ and $\rho_E = (|\Psi\rangle_E\langle\Psi| + |\Psi_\perp\rangle_E\langle\Psi_\perp|)/2$. Therefore, it is simple to find that the output state σ_{coh}^I (tracing over photon E) is exactly a mixture of the entangled state with the unpolarized noise (Werner state) [74]:

$$\sigma_{coh}^I = \frac{4F_{coh} - 1}{3}|\Psi_-\rangle\langle\Psi_-| + \frac{(1 - F_{coh})}{3}\mathbb{1} \otimes \mathbb{1}, \quad (5.2)$$

where the fidelity F_{coh} , that is the overlap with the singlet state $|\Psi_-\rangle_{AB}$, takes values $0 \leq F_{coh} \leq 1$ and reads:

$$F_{coh} = \frac{(1 - 3T)^2}{4(1 - 3T(1 - T))}. \quad (5.3)$$

The state is entangled only if $1/2 < F \leq 1$ and the concurrence [77] reads $C_{coh} = 2F_{coh} - 1$. If $F_{coh} < 1/2$ the entanglement is completely lost and the state (5.2) is separable. The explicit formula for concurrence is

$$C_{coh}^I = \max\left(0, \frac{3T^2 - 1}{2(1 - 3T(1 - T))}\right). \quad (5.4)$$

The probability of such situation is $P_{coh}^I = (T^2 + (T - R)^2 + R^2)/2$ and the condition for entanglement breaking channel is $T < 1/\sqrt{3}$. In order to achieve a maximal violation of Bell inequalities [73], we have to refer to the quantity B_{coh}^I given by the expression

$$B_{coh}^I = \frac{2\sqrt{2}T|1 - 2T|}{1 - 3T(1 - T)} \quad (5.5)$$

The violation appears only for $T > 0.68$, imposing a condition on the coupling even more strict.

More generally, all the result that will be presented can be directly extended for general passive coupling between two modes. It can be represented by Mach-Zehnder interferometer consisting to two unbalanced beam splitters (with transmissivity T_1 and T_2) and two phase shifts $-\phi$ and ϕ separately in arms inside the interferometer. All the results depends only on a single parameter: the probability T that the entangled photon will leave the coupling as the signal, which is

explicitly equal to:

$$T = T_1 + T_2 - 2T_1T_2 + \sqrt{T_1T_2R_1R_2} \cos 2\phi. \quad (5.6)$$

Thus all results, here simply discussed for a beam splitter, are valid for any passive coupling between two photons.

After the measurement of polarization on photon E , lets say by the projection on an arbitrary state $|\Psi\rangle_E$, the state of photons A, B is transformed into

$$\sigma_{coh}^{II} = \frac{1}{P_{coh}^{II}} ((T^2 + (T - R)^2)|T\rangle\langle T| + R^2|\Psi_\perp\Psi_\perp\rangle\langle\Psi_\perp\Psi_\perp|) \quad (5.7)$$

where the state $|T\rangle$ represents the unbalanced singlet state:

$$|T\rangle = \frac{1}{\sqrt{T^2 + (T - R)^2}} (T|\Psi\Psi_\perp\rangle - (T - R)|\Psi_\perp\Psi\rangle) \quad (5.8)$$

and $P_{coh}^{II} = T^2 + (T - R)^2 + R^2$. Calculating the concurrence as measure of entanglement, we found

$$C_{coh}^{II} = \frac{T|2T - 1|}{1 - 3(1 - T)T} \quad (5.9)$$

which is always larger than zero if $T \neq 0, 1/2$. It is worth notice that, irrespective to polarization noise in the qubit E , it is possible to probabilistically localized back to the original photon pair A and B a non-zero entanglement for all $T \neq 0, 1/2$.

A basic principle can be understood by comparing Eq. (5.2) and Eq. (5.7). The unpolarized noise in Eq. (5.2) has been transformed to a fully correlated polarized noise in Eq. (5.7) just by the measurement on E . This measurement can be arbitrary and does not depend on the coupling strength T . Thus, it is not necessary to estimate the channel coupling before the measurement. The positive result comes from the observation that a fully correlated and polarized noise is less destructive to maximal entanglement than the completely depolarized noise. Further, the entanglement localization effect persists even if an arbitrary phase or amplitude damping channel affects photon E after the coupling. If there is still a preferred basis in which the same classical correlation can be kept, it is sufficient for the entanglement localization. Unfortunately, the localized state is entangled but the localization itself is not enough to produce a state violating Bell inequalities. The maximal Bell factor B_{coh}^{II} is identical to (5.5) although the state has completely changed its structure.

However if T is known then the entanglement of state (5.7) and the Bell

inequality violation can be further increased by the single-copy distillation [79, 98, 88]. First, a local polarization filter can be used to get the balanced singlet state in the mixture. An explicit construction of the single local filter at Bob's side is given by $|\Psi\rangle \rightarrow (T-R)/T|\Psi\rangle, |\Psi_{\perp}\rangle \rightarrow |\Psi_{\perp}\rangle$ for $T > 1/3$. If $T < 1/3$ then a different filtering $|\Psi\rangle \rightarrow |\Psi\rangle, |\Psi_{\perp}\rangle \rightarrow T/(T-R)|\Psi_{\perp}\rangle$ has to be applied. Thus the Werner state (5.2) is conditionally transformed to a maximally entangled mixed state (MEMS)[99, 100, 101, 102]:

$$\frac{((T-R)^2|\Psi_{-}\rangle\langle\Psi_{-}| + R^2|\Psi_{\perp}\Psi_{\perp}\rangle\langle\Psi_{\perp}\Psi_{\perp}|)}{(T-R)^2 + R^2} \quad (5.10)$$

where the probability of success is given by $(T-R)^2 + R^2$. Due to symmetry, the same situation arises if the state $|\Psi_{\perp}\rangle$ is detected, just replacing the state $\Psi \leftrightarrow \Psi_{\perp}$. If the local filtering on Bob's side is applied according to the projection, it is possible to reach the MEMS with twice of success probability. Now, a difference between Eq.(5.10) and Eq. (5.2) is only in an additive fully correlated polarized noise. Such result can be achieved by an operation on the photon B , while a processing on other photon is not required.

Further local filtration performed on both photons A and B can give maximal entanglement achievable from a single copy. Both Alice and Bob should implement the filtration $|\Psi\rangle \rightarrow |\Psi\rangle$ and $|\Psi_{\perp}\rangle \rightarrow \sqrt{\epsilon}|\Psi_{\perp}\rangle$, where $0 < \epsilon \leq 1$. The filtered state is then

$$\sigma_{coh}^{III} = \frac{1}{4P_{coh}^{III}} (\epsilon(2T-1)^2|\Psi_{-}\rangle\langle\Psi_{-}| + \epsilon^2(1-T)^2|\Psi_{\perp}\Psi_{\perp}\rangle\langle\Psi_{\perp}\Psi_{\perp}|) \quad (5.11)$$

where $P_{coh}^{III} = (\epsilon(2T-1)^2 + \epsilon^2(1-T)^2)/4$ is probability of success. The state has the following concurrence for $T \neq 0, 1/2$

$$C_{coh}^{III}(\epsilon) = \frac{1}{1 + \epsilon \frac{(1-T)^2}{2(1-2T)^2}} \quad (5.12)$$

As ϵ goes to zero, the concurrence approaches unity, except for $T = 0, 1/2$, where it vanishes. Thus we can get entanglement arbitrarily close to its maximal value for any T (except $T = 0, 1/2$). For $T = 1/2$, it could not appear due to bunching effect between the photons at the beam splitter. Such result can be achieved since we can completely eliminate the fully correlated polarized noise, which is actually completely orthogonal to the single state $|\Psi_{-}\rangle$. We stress once again that maximal entanglement was probabilistically approached irrespective to the initial polarization noise of the photon E , just by its single-copy localization measurement and single-copy distillation.

If $\epsilon \rightarrow 0$ we get simply $B_{coh}^{III} = 2\sqrt{2}$ for any T , except $T = 0, 1/2$. Since the maximal entanglement allows ideal teleportation of unknown state we can conclude that the coherent linear coupling with the photon even in an unknown state could be practically probabilistically reversed. It is interesting to make a comparison with the deterministic localization procedure. To achieve it, we need perfect control of the state of photon E before the coupling. We can know it either a priori or by a measurement on the more complex systems predicting pure state of E . Being $|\Psi\rangle_E$ the state of E after coupling, three-photon state is proportional to $|\Psi\rangle_A (T|\Psi_\perp\Psi\rangle_{BE} - R|\Psi\Psi_\perp\rangle_{BE}) - (T - R)|\Psi_\perp\Psi\Psi\rangle_{ABE}$. This belongs to non-symmetrical W-state, rather than to GHZ states, therefore the maximal entanglement can not be obtained deterministically. It can be done by the projection on $|\Psi\rangle_E$ followed by the single-copy distillation. From this point of view, the unpolarized noise of photon E does not qualitatively change the result of the localization, but only decreases the success rate.

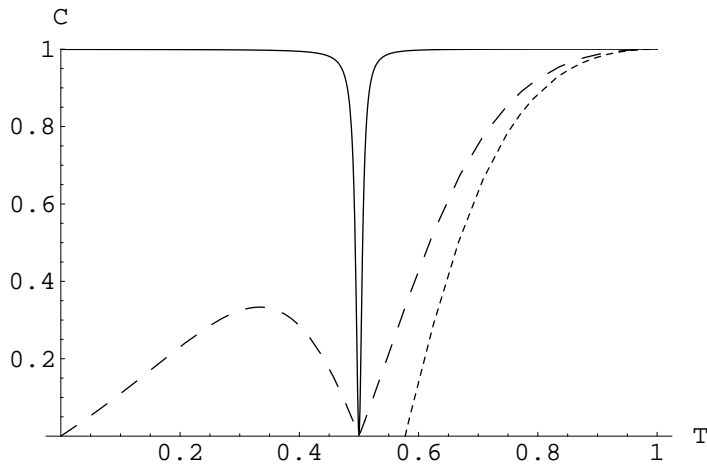


Figure 5.3: Concurrence for indistinguishable photon E ($p = 1$): C_{coh}^I without measurement (dotted), C_{coh}^{II} with measurement (dashed), C_{coh}^{III} with measurement and LOCC filtration (full), for $\epsilon = 0.005$.

5.2.2 Partially incoherent coupling

Up to now, we have assumed that both photons B and E are indistinguishable in the linear coupling. On the other hand, if they are partially or fully incoherent (in principle distinguishable), then it is in principle possible to perfectly filter out surrounding photons from the signal photons after the coupling. Although they are in principle partially or fully distinguishable, any realistic attempt to discriminate them would be typically too noisy to offer such information. Here we are interested in the opposite situation, when distinguishable photon B and

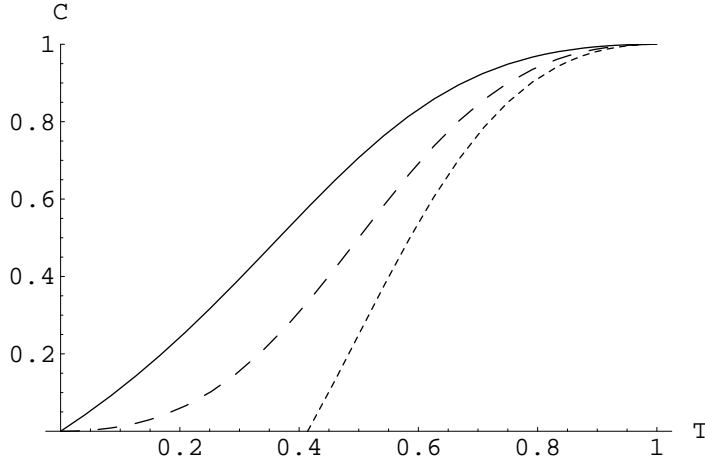


Figure 5.4: Concurrence for distinguishable photon ($p = 0$): C_{inc}^I without measurement (dotted), C_{inc}^{II} with measurement (dashed), C_{inc}^{III} with measurement and LOCC filtration (full)

surrounding photon E cannot be practically distinguished after the coupling. It is an open question whether the entanglement localization method can still help us. For simplicity, let us assume a mixture of the previous case with a situation where both the photons B and E are completely distinguishable. The state is mixture $p\sigma_{coh} + (1-p)\rho_{inc}$, where only with probability p the photons are indistinguishable. After the coupling and tracing over photon E , the output state is once more a Werner state (5.2) with fidelity

$$F(p) = \frac{(4p + 5)T^2 - 2(2p + 1)T + 1}{4(1 - (2 + p)T(1 - T))} \quad (5.13)$$

and success probability $P(p) = 1 - (2 + p)T(1 - T)$. The concurrence is given by $C(p) = 2F(p) - 1$. The entanglement between A and B is lost if

$$p > \frac{T^2 + 2T - 1}{2T(1 - T)} \quad (5.14)$$

and thus for $T < \sqrt{2} - 1$, the entanglement between A and B is lost for any p . The maximal Bell factor

$$B(p) = 2\sqrt{2}T \frac{|T - p(1 - T)|}{1 - (p + 2)(1 - T)T} \quad (5.15)$$

gives violation of Bell inequalities only if $p \in [0, 1]$ satisfies

$$p < \sqrt{2} + \frac{1}{1 - T} - \frac{1 + \sqrt{2}}{T}. \quad (5.16)$$

Let us discuss first the entanglement localization for the fully distinguishable photon case ($p = 0$). In this limit, after the coupling the fidelity reads:

$$F_{inc} = \frac{5T^2 - 2T + 1}{4(1 - 2T(1 - T))}, \quad (5.17)$$

and the concurrence and the maximal violation of Bell inequalities are

$$C_{inc}^I = \frac{T^2 + 2T - 1}{2(1 - 2T(1 - T))}, \quad B_{inc}^I = 2\sqrt{2} \frac{T^2}{T^2 + (1 - T)^2}. \quad (5.18)$$

The concurrence vanishes for $T < \sqrt{2} - 1$ and the violation of Bell inequalities disappears for $T < 1 + \frac{1}{\sqrt{2}} \left(1 - \sqrt{1 + \sqrt{2}}\right) \approx 0.608$. In both cases, the thresholds are lower than for the coherent coupling; the coherence of photon E leads to less robust transmission of the quantum resources.

If the projection on $|\Psi\rangle_E$ is performed on the environmental photon after the coupling, the resulting state reads

$$\rho_{inc}^{II} = \frac{1}{P_{inc}^{II}} \left(\frac{T^2}{2} |\Psi_{-}\rangle_{AB} \langle\Psi_{-}| + \frac{R^2}{2} |\Psi_{\perp}\rangle_A \langle\Psi_{\perp}| \otimes \frac{\mathbb{1}_B}{2} \right) \quad (5.19)$$

where $P_{inc}^{II} = (T^2 + R^2)/2$. Clearly, the additive noisy term in the Eq.(5.19) is separable and the full correlation in the partially polarized noise (5.7) does not arise here, in comparison with the fully coherent case. Except for $T = 0$, this state is exhibiting non-zero concurrence

$$C_{inc}^{II} = \frac{T^2}{2T^2 - 2T + 1} \quad (5.20)$$

which is a decreasing function of T . The state just after the localization does not violate Bell inequalities, since the maximal Bell factor is the same as after the mixing $B_{inc}^{II} = B_{inc}^I$. Similarly to the previous discussion, projecting on $|\Psi_{\perp}\rangle_E$, we get an identical state, only replacing $\Psi \leftrightarrow \Psi_{\perp}$. This means that even for completely non-interfering photons B and E , a polarization measurement on the photon E can localize entanglement back to photons A and B . To approach it with maximal success rate, local unitary transformations doing $\Psi \leftrightarrow \Psi_{\perp}$ have to be applied if $|\Psi_{\perp}\rangle$ is measured. Similarly to previous coherent case, the photon E is not affected by the amplitude or phase damping channel. It is only important to keep a preferred basis without any noise influence.

The physical mechanism which models the localization process for incoherent coupling is different from the previous case. Here, the three-photon mixed state

after the coupling is proportional to

$$T^2|\Psi_{-}\rangle_{AB}\langle\Psi_{-}| \otimes \mathbb{1}/2_E + R^2|\Psi_{-}\rangle_{AE}\langle\Psi_{-}| \otimes \mathbb{1}/2_B \quad (5.21)$$

describing just a random swap of the photons B and E at the beam splitter. Although there is no correlation generated by the coupling between photons A and B , contrary to previous case, still a correlation between photons A and E will appear in the second part of expression due to the initial entangled state. It is used to conditionally transform the locally completely depolarized state of photon A to a fully polarized state. Of course, it does not have any impact on the local state of photon B . But it is fully enough to localize entanglement for any T after the projection on photon E . It is rather a non-local correlation effect where the polarization noise is corrected not at photon B but at photon A .

The entanglement can be further enhanced using local filtration and classical communication; in the limit $\epsilon \rightarrow 0$, it approaches the concurrence $C_{inc}^{III} = \sqrt{C_{inc}^{II}}$, at cost of a decreasing success rate. Optimal filtering is then given by

$$\begin{aligned} |\Psi_{\perp}\Psi\rangle &\rightarrow \frac{T}{\sqrt{2T^2 - 2T + 1}}|\Psi_{\perp}\Psi\rangle, \\ |\Psi_{\perp}\Psi_{\perp}\rangle &\rightarrow \epsilon|\Psi_{\perp}\Psi_{\perp}\rangle \end{aligned} \quad (5.22)$$

whereas all other basis states are preserved. But, contrary to the case of two perfectly interfering photons, maximal entanglement cannot be approached for any $T < 1$. This is a cost of incoherence in the entanglement localization for distinguishable photons. Of course, the collective protocols can be still used, since all entangled two-qubit state are distillable to maximally entangled state [79].

A maximal value of the Bell factor

$$B_{inc}^{III} = 2\sqrt{1 + \frac{T^2}{T^2 + (1 - T)^2}} \quad (5.23)$$

can be achieved if $\epsilon \rightarrow 0$ for any T . Although the maximal violation of Bell inequalities is greater than 2 the full entanglement cannot be recovered at any single copy. The partial violation of Bell inequalities guaranties important quantum mechanical properties, for example, the security of quantum key distribution.

Also here it is instructive to make a comparison with the case in which the photon E is in the known pure state $|\Psi\rangle_E$. Then after the coupling the three-photon state is proportional to $T^2|\Psi_{-}\rangle_{AB}\langle\Psi_{-}| \otimes |\Psi\rangle_E\langle\Psi| + R^2|\Psi_{-}\rangle_{AE}\langle\Psi_{-}| \otimes$

$|\Psi\rangle_B\langle\Psi|$ and after the projection on $|\Psi\rangle_E$, it transforms to $T^2|\Psi_-\rangle_{AB}\langle\Psi_-| + \frac{1}{2}R^2|\Psi_\perp\rangle_A\langle\Psi_\perp| \otimes |\Psi\rangle_B\langle\Psi|$. Since both the contributions are not orthogonal there is no local filtration procedure which could filter out the $|\Psi_-\rangle_{AB}$ from the noise contribution. Therefore, although we could have a complete knowledge about pure state of the photon E , its incoherence does not allow to achieve maximal entanglement from the single copy distillation.

For the mixture of both the distinguishable and indistinguishable photons, the concurrence after the measurement is

$$C^I(p) = \max\left(0, \frac{|(1+p)T^2 - pT|}{1 - (2+p)T(1-T)}\right), \quad (5.24)$$

which is positive if $p \neq T/(1-T)$ and

$$p < \frac{1-T}{T} + \frac{T}{1-T}. \quad (5.25)$$

Except $T = 0, p/(1+p)$, the last condition is always satisfied since right side has minimum equal to two. Even if the noise is a mixture of distinguishable and indistinguishable photons, it is possible to localize entanglement just by a measurement for almost all the cases. After the application of LOCC polarization filtering, the concurrence can be enhanced up to

$$C^{III}(p, \epsilon) = \frac{2T^2|T - p(1-T)|}{\sqrt{1 - 2(1+p)(1-T)T(\epsilon(1-T)^2 + 2T^2)}}. \quad (5.26)$$

In the limit of $\epsilon \rightarrow 0$, it approaches

$$C^{III}(p) = \max\left(0, \frac{|T - p(1-T)|}{\sqrt{1 - 2(1+p)T(1-T)}}\right) \quad (5.27)$$

which is plotted at the top of FIG. 5.5. The maximal entanglement can be only induced for $p = 1$. Comparing both the discussed cases of the indistinguishable and distinguishable photons, it is evident that it can be advantageous to induce indistinguishability. For example, if they are distinguishable in time, then spectral filtering can help us to make them more distinguishable and consequently, the entanglement can be enhanced more by local filtering.

For partially indistinguishable photons given by parameter p , after the measurement stage we get the same value of the Bell factor as after the mixing stage $B^{II}(p) = B^I(p)$. For enhancement of the Bell factor the local filtration operations is also essential. We apply the two stage filtration operations as stated previously. If the filtration parameter

$$\epsilon \in \left(\frac{X_1 - X_2}{X_3}, \frac{X_1 + X_2}{X_3} \right) \quad (5.28)$$

where $X_1 = 2T^2\sqrt{1 - 2(p+1)(1-T)T}$, $X_2 = 2T^2|T - p(1-T)|$, $X_3 = (T-1)^2\sqrt{1 - 2(p+1)(1-T)T}$, then we get following Bell factor

$$B^{III}(p, \epsilon) = \frac{4\sqrt{2}T^2|p(T-1) + T|}{\sqrt{2(p+1)(T-1)T+1}(2T^2 + (T-1)^2\epsilon)} \quad (5.29)$$

otherwise we get

$$B^{III}(p, \epsilon) = \frac{2\sqrt{\frac{4T^4(p(T-1)+T)^2}{2(p+1)(T-1)T+1} + ((T-1)^2\epsilon - 2T^2)^2}}{2T^2 + (T-1)^2\epsilon}. \quad (5.30)$$

The particular cases of Bell factors given previously can be obtained from the above relations setting $p = 0$ ($p = 1$) for incoherent (coherent) coupling and additionally the maximal value of the Bell factor is obtained if ϵ goes to zero. In order to get violation of the Bell inequalities $B^{III}(p, \epsilon) > 2$ the filtration parameter needs to be for the (5.29)

$$\epsilon < \frac{T^2(p(T-1) + T)^2}{2(T-1)^2(2(p+1)(T-1)T+1)} \quad (5.31)$$

and for the (5.30)

$$\epsilon < \frac{2T^2}{(T-1)^2} \left(\frac{\sqrt{2}|p(T-1) + T|}{\sqrt{2(p+1)(T-1)T+1}} - 1 \right). \quad (5.32)$$

In both the cases, value of ϵ should rapidly decrease as T is smaller. In other words, it means that for a given ϵ , the state violates Bell inequalities only if p is sufficiently large. For any p and T , there is always some $\epsilon > 0$ below the region given by (5.28), therefore as $\epsilon \rightarrow 0$, the maximal violation

$$B^{III}(p) = 2\sqrt{1 + \frac{(p(T-1) + T)^2}{2(p+1)(T-1)T+1}}. \quad (5.33)$$

comes from the Eq. (5.29) since it is higher than the limit expression from Eq. (5.30). The maximal violation of Bell inequalities is plotted at the bottom of FIG. 5.5. Generally, for $\epsilon > 0$ we have to compare the (5.29) and (5.30) to find out which gives higher $B^{III}(p)$.

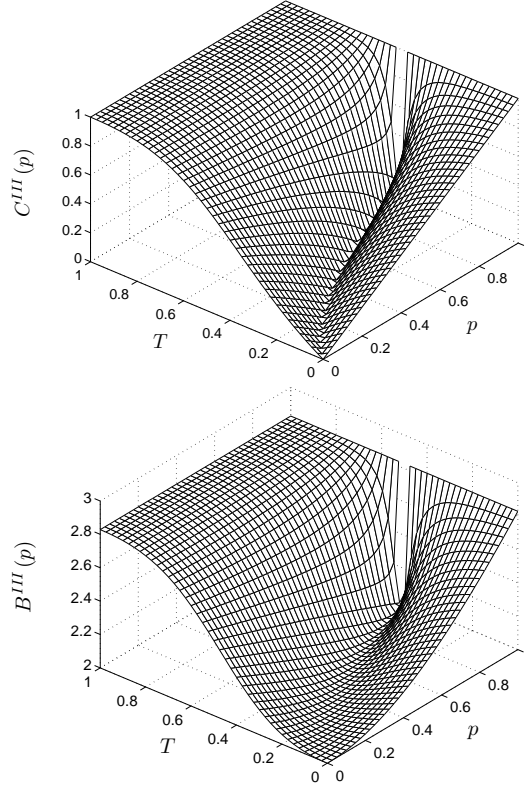


Figure 5.5: Maximal concurrence and maximal violation of Bell inequalities for the localized state.

5.3 Experimental Implementation

Let us now describe the experimental implementation of the localization protocol both for the fully incoherent and partially coherent coupling regime.

5.3.1 Experimental setup

The main source of the experiment is a Ti : Sa mode-locked pulsed laser with wavelength (wl) $\lambda = 795nm$, pulse duration of $180fs$ and repetition rate $76MHz$: FIG.5.6. A small portion of this laser, got with a low reflectivity mirror M , generates the single photon over the mode k_E using an attenuator (ATT). The transformation used to map the state $|H\rangle_E$ into $\rho_E = \frac{I_E}{2}$ is achieved either adopting a Pockels cell driven by a sinusoidal signal, either through a stochastically rotated $\lambda/2$ waveplate inserted on the mode k_E during the experiment [103]. The main part of the laser through a second harmonic generation (SHG) where a bismuth borate (BiBO) crystal [104] generates a UV laser beam having wave-vector k_p and wl $\lambda_p = 397.5nm$ with power equal to $800mW$. A dichroic mirror (DM) separates the residual beam at λ left after the SHG process from the UV laser beam.

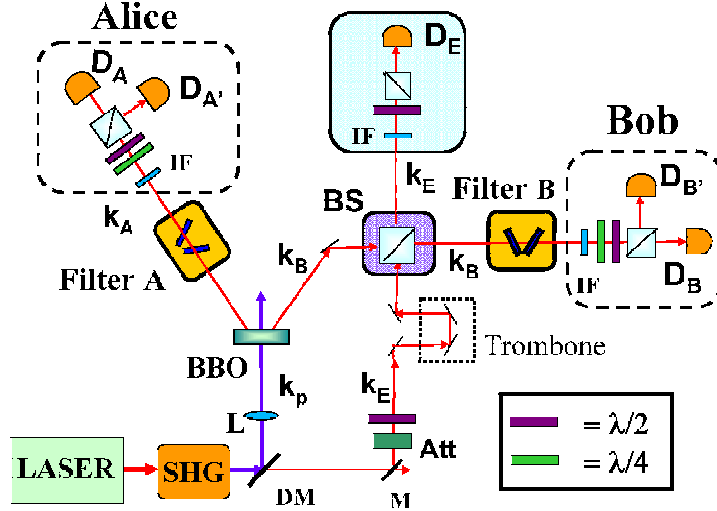


Figure 5.6: Schematic representation of the experimental setup. The dashed boxes indicate the polarization analysis setup adopted by Alice and Bob.

This field pump a 1.5mm thick non-linear crystal of β -barium borate (BBO) cut for type II phase-matching that generates polarization maximally entangled pairs of photons. The spatial and temporal walk-off is compensated by inserting a $\frac{\lambda}{2}$ waveplate and a 0.75 mm thick BBO crystal on each output mode k_A and k_B [7]. The photons of each pair are emitted with equal wavelength $\lambda = 795\text{nm}$ over the two spatial modes k_A and k_B . In order to couple the noise with the signal, the photons on modes k_B and k_E are injected in the two input arms of an unbalanced beam splitter BS characterized by transmissivity T and reflectivity $R = 1 - T$. A mutual delay Δt , micrometrically adjustable by a two-mirrors optical "trombone" with position settings $Z = 2c\Delta t$, can change the temporal matching between the two photons. Indeed, the setting value $Z = 0$ corresponds to the full overlap of the photon pulses injected into BS , i.e., to the maximum photon interference. On output modes $k_{B'}$ and $k_{E'}$ the photons are spectrally filtered adopting two interference filters (IF) with bandwidth equal to 3nm , while on mode k_A the IF has a bandwidth of 4.5nm .

Let us now describe how the measurement on the environment has been experimentally carried out. According to the protocol described above, the photon propagating on mode $k_{E'}$ is measured after a polarization analysis realized through a $\frac{\lambda}{2}$ and a polarizing beam splitter (PBS). In order to restore the optimum value of entanglement according to theory, a filtering system has been inserted on k_A and $k_{B'}$ modes. As shown in FIG.5.6, the filtering is achieved by two sets of glass positioned close to their Brewster's angle, in order to attenuate one polarization in comparison to its orthogonal. The attenuation over the mode k_i for the H -polarization (V -polarization) reads A_i^H (A_i^V). By tuning the incidence

angle, different values of attenuation $\{A_i^j\}$ can be achieved. Finally, to verify the working of the overall protocol, the emerging photons on modes k_A and $k_{B'}$ are analyzed in polarization through a $\frac{\lambda}{2}$ waveplate (wp), a $\frac{\lambda}{4}$ and a PBS. Then the photons are coupled to a single mode fiber and detected by single photon counting module (SPCM) $\{D_A, D_{A'}, D_{B'}, D_B\}$. The output signals of the detectors are sent to a coincidence box interfaced with a computer, which collects the double coincidence rates ($[D_A, D_B]$, $[D_A, D_{B'}]$, $[D_{A'}, D_B]$, $[D_{A'}, D_{B'}]$) and triple coincidence rates ($[D_A, D_B, D_E]$, $[D_A, D_{B'}, D_E]$, $[D_{A'}, D_B, D_E]$, $[D_{A'}, D_{B'}, D_E]$). The detection of triple coincidence ensures the presence of one photon per mode after the BS . In order to determine all the elements of the two-qubit density matrix, an overcomplete set of observables is measured by adopting different polarization settings of the $\frac{\lambda}{2}$ wp and $\frac{\lambda}{4}$ wp positions [105]. The uncertainties on the different observables have been calculated through numerical simulations of counting fluctuations due to the Poissonian distributions. Here and after, we will distinguish the experimental density matrix from the theoretical one by adding a "tilde" $\tilde{\cdot}$.

As first experimental step, we have characterized the initial entangled state generated by the NL crystal on mode k_A and k_B , that is the signal to be transmitted through the noisy channel. The overall coincidence rate is equal to about 8.000 coincidences per second. The experimental quantum state tomography of $\tilde{\rho}_{AB}^{in}$ is reported in FIG.5.8-a, to be compared with the theoretical one $\rho_{AB}^{in} = |\Psi^{in}\rangle_{AB} \langle\Psi^{in}|_{AB}$, where $|\Psi^{in}\rangle = (|HV\rangle + i|VH\rangle)/\sqrt{2}$ (FIG.5.7-a). Although the generated state differs from the singlet state, all the conclusions from the previous section remains valid. We found a value of the concurrence $\tilde{C}_{in} = (0.869 \pm 0.005)$ and a linear entropy $\tilde{S}_{in} = (0.175 \pm 0.005)$, where the uncertainty on the concurrence has been calculated applying the Monte-Carlo method on the experimental density matrix. The fidelity with the entangled state $|\Psi^{in}\rangle_{AB}$ is $\mathcal{F}(\tilde{\rho}_{AB}^{in}, |\Psi^{in}\rangle_{AB}) = \langle\Psi^{in}|_{AB} \tilde{\rho}_{AB}^{in} |\Psi^{in}\rangle_{AB} = (0.915 \pm 0.002)$. The discrepancy between theory and experiment is mainly attributed to double pairs emission. Indeed by subtracting the accidental coincidences we obtain a concurrence equal to $\tilde{C}'_{in} = (0.939 \pm 0.006)$ and a linear entropy of $\tilde{S}'_{in} = (0.091 \pm 0.006)$. The fidelity with the entangled state $|\Psi^{in}\rangle_{AB}$ is then equal to $F'(\tilde{\rho}_{AB}^{in}, |\Psi^{in}\rangle_{AB}) = (0.949 \pm 0.003)$. Minor sources of imperfections related to the generation of our entangled state are the presence of spatial and temporal walk-off due to the non linearity of the BBO crystal as well as a correlation in wavelength of the generated pairs of photons.

5.3.2 Incoherent coupling

The experiment with distinguishable photons has been achieved by injecting a single photon E with a randomly chosen mutual delay with photon B of $\Delta t \gg \tau_{coh} = 300 fs$. We note that the resolution time t_{det} of the detector is $t_{det} \gg \Delta t$, hence it is not technologically possible to individuate whether the detected photon belongs to the environment or to the entangled pair. To carry out the experiment we adopted a beam splitter with $T = 0.40$ which, according to the theoretical prediction (see FIG. 5.4), allows to study the entanglement localization process. Since multi-photon contributions represent the main source of imperfections in our calculations, we have subtracted their contributions in all the experimental data reported for the density matrices of each step of the protocol.

I) Mixing

Without any access to the environmental photon, after the mixing on the BS , once there is one photon per output mode, the theoretical input state $\rho^{in} = |\Psi^{in}\rangle\langle\Psi^{in}|$ evolves into a noisy state represented by the density matrix ρ_{inc}^I , written in the basis $\{|HH\rangle, |HV\rangle, |VH\rangle, |VV\rangle, \}$ as:

$$\rho_{inc}^I = \frac{1}{4P_{inc}^I} \begin{pmatrix} \alpha & 0 & 0 & 0 \\ 0 & \beta & i\xi & 0 \\ 0 & -i\xi & \gamma & 0 \\ 0 & 0 & 0 & \delta \end{pmatrix} \quad (5.34)$$

with $\alpha = \delta = R^2$, $\beta = \gamma = R^2 + 2T^2$, $\xi = 2T^2$ and $P_{inc}^I = R^2 + T^2$, where $R = 1 - T$ indicates the reflectivity of the beam splitter. This matrix, shown in FIG.(5.7-I), exhibits theoretically concurrence

$$C_{inc}^I = \max(0, \frac{2T^2 - R^2}{2P_I}). \quad (5.35)$$

Because of the interaction with noise, ρ_{inc}^I does not exhibit entanglement ($C_{inc}^I = 0$) and is highly mixed with linear entropy equal to $S_{inc}^I = 0.90$. Afterwards we analyze experimentally how the entangled state is corrupted due to the coupling with the photon E . In this case no-polarization selection is performed on mode k_E . The experimental density matrix $\tilde{\rho}_{inc}^I$ is shown in FIG.(5.8-I). As expected, it exhibits $\tilde{C}_{inc}^I = 0$, and $\tilde{S}_{inc}^I = (0.89 \pm 0.01)$. The fidelity with theory is high: $\tilde{F}_{inc}^I = F(\tilde{\rho}_{inc}^I, \rho_{inc}^I) = (0.997 \pm 0.006)$, with $F(\rho, \sigma) = \text{Tr}^2 \left[(\sqrt{\rho\sigma}\sqrt{\rho})^{1/2} \right]$. In this case, due to the coupling the entanglement is completely redirected and no quantum distillation protocol can be applied to restore entanglement between

photons A and B .

II) Measurement

As no selection has been performed on the photon E before the coupling, a multi-mode photon E interacts with the entangled photon B . After the interaction, a single mode fiber has been inserted on the output mode of the BS in order to select only the output mode connected with the entanglement breaking. Let us consider the case in which the photon on mode k_E is measured in the state $|H\rangle_E$. After the measurement, the density matrix ρ_{inc}^I evolves into an entangled one described by the density matrix ρ_{inc}^{II}

$$\rho_{inc}^{II} = \frac{1}{4P_{inc}^{II}} \begin{pmatrix} 0 & 0 & 0 & 0 \\ 0 & \beta & i\xi & 0 \\ 0 & -i\xi & \gamma & 0 \\ 0 & 0 & 0 & \delta \end{pmatrix} \quad (5.36)$$

where $\delta = R^2$, $\beta = T^2$, $\gamma = R^2 + T^2$, $\xi = T^2$: FIG.(5.7-II). In this case the concurrence reads

$$C_{inc}^{II} = \frac{T^2}{2P_{inc}^{II}} \quad (5.37)$$

with $P_{inc}^{II} = P_{inc}^I/2$. The entanglement is localized back for all the values of $T \neq \{0, \frac{1}{2}\}$ but, as shown in the graph, the elements of the matrix are fairly unbalanced. According to theory, we expect a localization of the entanglement with $C_{inc}^{II} = 0.32$, and success rate $P_{inc}^{II} = 0.27$. Experimentally we obtain $\tilde{C}_{inc}^{II} = (0.19 \pm 0.02) > 0$, a fidelity with the theoretical density matrix ρ_{inc}^{II} equal to $\tilde{F}_{inc}^{II} = (0.96 \pm 0.03)$, while the mixedness of the state decreases $\tilde{S}_{inc}^{II} = (0.72 \pm 0.02)$ to be compared to theoretical prediction $S_{inc}^{II} = 0.74$. This is achieved at the cost of a probabilistic implementation where the probability of success reads: $\tilde{P}_{inc}^{II} = (0.26 \pm 0.01)$.

III) Filtration

The filtration is introduced onto the mode k_A and k_B , attenuating the vertical polarization, in order to increase the concurrence and symmetrizing the density matrix by a lowering of the $|VV\rangle\langle VV|$ component in ρ_{inc}^{II} : FIG.(5.7-II). After filters F_A and F_B , the density matrix reads:

$$\rho_{inc}^{III} = \begin{pmatrix} 0 & 0 & 0 & 0 \\ 0 & \epsilon\beta & i\epsilon\xi & 0 \\ 0 & -i\epsilon\xi & \epsilon\beta & 0 \\ 0 & 0 & 0 & \epsilon^2\delta \end{pmatrix} \quad (5.38)$$

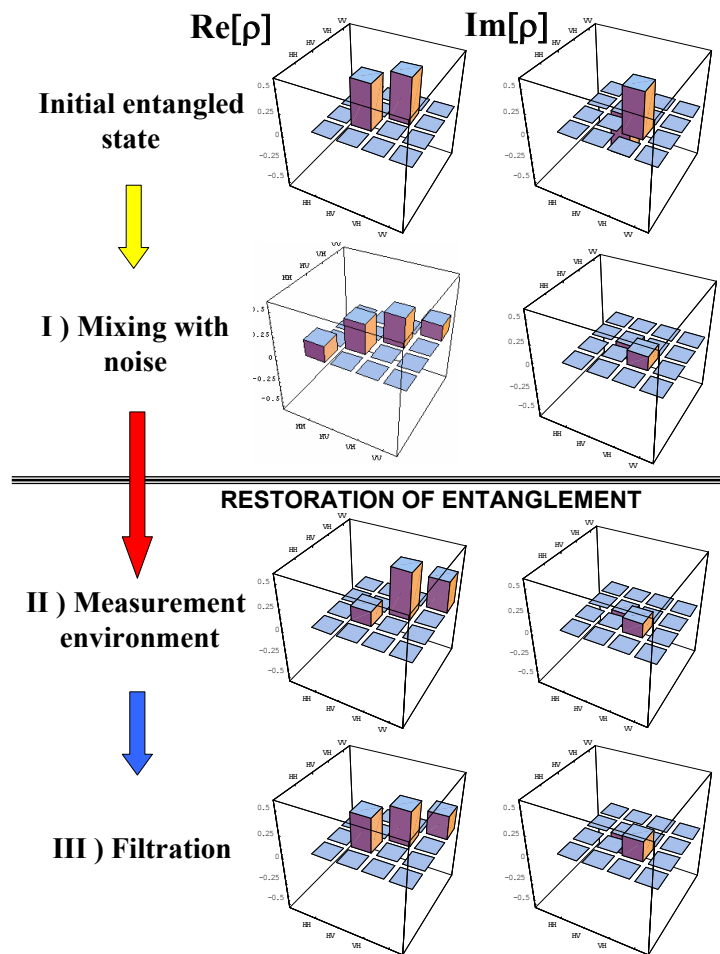


Figure 5.7: Theoretical density matrix for distinguishable photons, enlightening the evolution of ρ through each step of the entanglement localization protocol.

where $\beta = T^2$, $\delta = R^2$, $\xi = \frac{T^3}{\sqrt{T^2+R^2}}$. The concurrence reads

$$C_{inc}^{III} = \frac{2\epsilon\xi}{2\epsilon\beta + \epsilon^2\delta} \quad (5.39)$$

while the probability of success of the protocol is equal to $P_{inc}^{III} = 2\epsilon\beta + \epsilon^2\delta$. The intensity of filtration is quantified by the parameter $0 < \epsilon \leq 1$, connected to the attenuation of V polarization. The concurrence has a limit for asymptotic filtration ($\epsilon \rightarrow 0$) lower than unity and maximal entanglement cannot be approached. Of course, the collective protocols can be still used, since all entangled two-qubit state are distillable to a singlet one. By setting the following attenuation values $A_A^V = 0.33$, $A_A^H = 1$, the theory predicts the achievement of ρ_{inc}^{III} (FIG.(5.7-III))

with the mixedness $S_{inc}^{III} = 0.76$ and the concurrence $C_{inc}^{III} = 0.42$. The probability of success of the filtration operation is $P_{inc}^{III} = 0.43$ leading to an overall probability of success of the entanglement restoration $P_{total} = P_{inc}^{II} P_{inc}^{III} = 0.12$. The highest concurrence value which can be obtained with the coupling $T = 0.40$ is equal to $C = 0.55$ for $P_{total} \rightarrow 0$. Experimentally we achieve the state shown in FIG.(5.8-III with a fidelity $\tilde{F}_{inc}^{III} = (0.89 \pm 0.06)$ and measure a concurrence equal to $\tilde{C}_{inc}^{III} = (0.28 \pm 0.02) > \tilde{C}_{inc}^{II}$ while $\tilde{P}_{inc}^{III} \tilde{P}_{inc}^{II} = (0.11 \pm 0.01)$ and $\tilde{S}_{inc}^{III} = (0.70 \pm 0.02)$. The experimental results shown above demonstrate the localization protocol validity, indeed a channel redirecting entanglement can be corrected to a channel preserving relatively large amount of the entanglement.

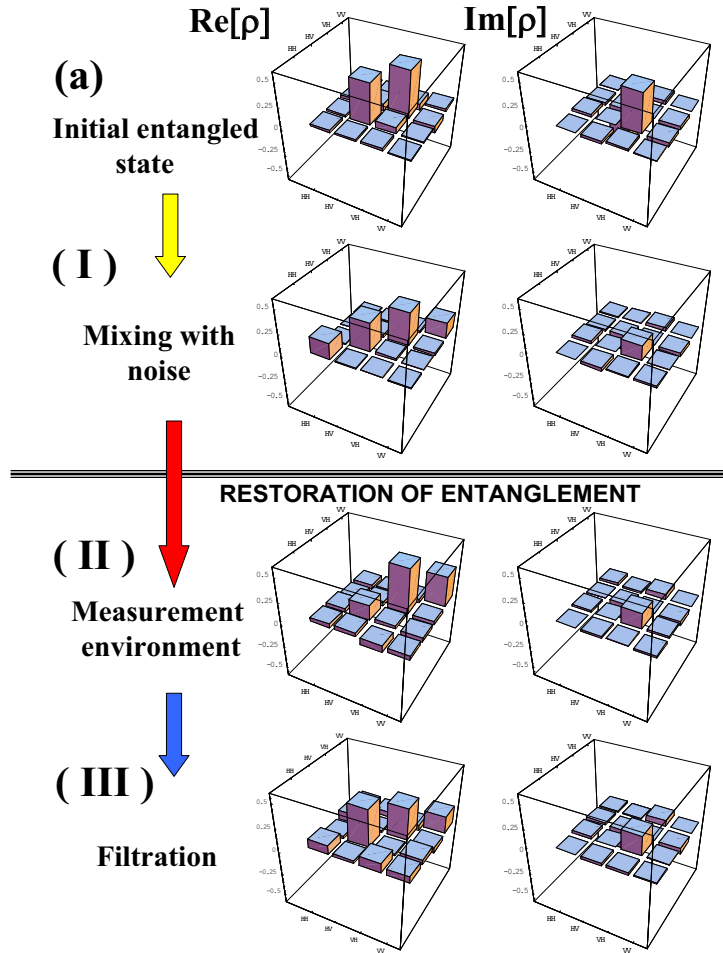


Figure 5.8: Experimental density matrix for distinguishable photons: **a)** $\tilde{\rho}^{in}$, **I)** $\tilde{\rho}_{inc}^I$, **II)** $\tilde{\rho}_{inc}^{II}$, **III)** $\tilde{\rho}_{inc}^{III}$. For each tomographic setting the measurement lasts from 5 s (**a**) to 30 minutes (**III**), the last case corresponding to about 500 triple coincidence. Contributions due to triple accidental coincidences have been subtracted from experimental data.

Let's explain the choice of introducing experimentally just one set of filtration instead of two. The glasses close to Brewster's angle attenuate the V polarization.

Let ϵ be the intensity of attenuation, the $|VH\rangle$ element of the density matrix will be attenuated by a factor $\sqrt{\epsilon}$. Even if the theory expects an element $|HH\rangle$ close to zero, in the experimental case we obtain a non-zero element due to the intensity of the coherent radiation, revealed by double photons contributions. Hence a filtration of ϵ on both modes, since it introduces an attenuation of ϵ on the element $|VV\rangle$ and of $\sqrt{\epsilon}$ on both the elements $|HV\rangle$ and $|VH\rangle$, would bring to a wider comparability between $|HH\rangle$ and $|HV\rangle$ elements, leading to a lower concurrence.

5.3.3 Coherent coupling

In order to exploit the regime where our localization protocol works best, we let the signal photon and the noise one be spatially, spectrally and temporal perfectly indistinguishable in the coupling process. A good spatial overlap is achieved by selecting the output modes through single mode fibers.

I) Mixing.

In the fully indistinguishable photons regime, we indicate with σ_{coh}^I the density matrix after the mixing on the *BS*, which is separable for $T < 1/\sqrt{3}$, as shown in FIG. 5.3. The output state is a mixture of the initial state $|\Psi^{in}\rangle\langle\Psi^{in}|$ and the fully mixed one [74]: FIG.5.9-I.

$$\sigma_{coh}^I = \frac{1}{4P_{coh}^I} \begin{pmatrix} \alpha & 0 & 0 & 0 \\ 0 & \beta & i\xi & 0 \\ 0 & -i\xi & \gamma & 0 \\ 0 & 0 & 0 & \delta \end{pmatrix} \quad (5.40)$$

with $\alpha = \delta = R^2$, $\beta = \gamma = T^2 + (T - R)^2$, $\xi = -T(T - R)$. The concurrence reads

$$C_{coh}^I = \frac{3T^2 - 1}{2P_{coh}^I}, \quad (5.41)$$

where $P_{coh}^I = 3T^2 - 3T - 1$.

II) Measurement.

A measurement is carried out on the environmental mode through the pro-

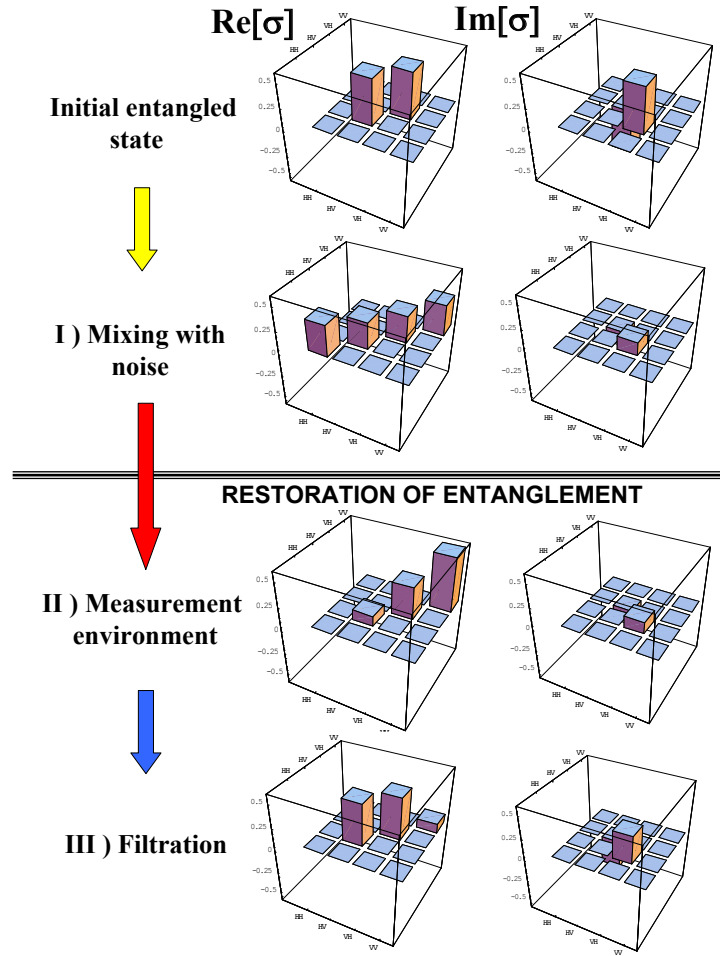


Figure 5.9: Theoretical density matrix for perfectly indistinguishable photons interacting on the BS .

jection on $|H\rangle_{E'}$. Thus the state σ_{coh}^I evolves into σ_{coh}^{II} :

$$\sigma_{coh}^{II} = \frac{1}{4P_{coh}^{II}} \begin{pmatrix} 0 & 0 & 0 & 0 \\ 0 & \beta & i\xi & 0 \\ 0 & -i\xi & \gamma & 0 \\ 0 & 0 & 0 & \delta \end{pmatrix} \quad (5.42)$$

with $\beta = T^2$, $\gamma = T^2 + (T - R)^2$, $\delta = R^2$, $\xi = -T(T - R)$. The state is conditionally transformed into a maximally entangled state (MEMS) [99]: see FIG.(5.10-II). In particular, it is found

$$C_{coh}^{II} = \frac{T|T - R|}{2P_{coh}^{II}} \quad (5.43)$$

and $P_{coh}^{II} = (T^2 + (T - R)^2 + R^2)/4$.

III) Filtration

Due to the strong asymmetry of σ_{coh}^{II} a filter is introduced either on Alice or Bob mode, depending on the value of T . If $T > |2T - 1|$, filter F_B acts on Bob mode, as $|H\rangle_B \rightarrow \frac{2T-1}{T}|H\rangle_B$, while if $T < |2T - 1|$, the filter acts on Alice mode, as $|V\rangle_A \rightarrow \frac{T}{2T-1}|V\rangle_A$. In order to increase the concurrence, a second filter is inserted on both Alice and Bob mode, which attenuates the vertical polarization component: $|V\rangle \rightarrow \sqrt{\epsilon}|V\rangle$. The filters F_A and F_B transform the density matrix into σ_{coh}^{III} :

$$\sigma_{coh}^{III} = \frac{1}{4P_{coh}^{III}} \begin{pmatrix} 0 & 0 & 0 & 0 \\ 0 & \epsilon\alpha & i\epsilon\alpha & 0 \\ 0 & -i\epsilon\alpha & \epsilon\alpha & 0 \\ 0 & 0 & 0 & \epsilon^2\delta \end{pmatrix} \quad (5.44)$$

where $\alpha = T^2$, $\delta = \left(\frac{TR}{R-T}\right)^2$, for $T < |2T - 1|$ and $\alpha = (2T - 1)^2$, $\delta = R^2$, for $T > |2T - 1|$: FIG.5.9-II. The concurrence has value

$$C_{coh}^{III} = \frac{2\epsilon\alpha}{2\epsilon\alpha + \epsilon^2\delta} \quad (5.45)$$

while the probability reads $P_{coh}^{III} = (2\epsilon\alpha + \epsilon^2\delta)/4$. Hence in the limit of asymptotic filtration ($\epsilon \rightarrow 0$), the concurrence reaches unity except for $T = 1/2$ [99].

5.3.4 Mixture of coherent and incoherent coupling

Let us now face up to a model which contemplates a situation close to the experimental one. In fact a perfect indistinguishability between the photons B and E is almost impossible to achieve experimentally. We consider the density matrix τ_{AB} of the state shared between Alice and Bob after the coupling, as a mixture arising from coupling with a partially distinguishable noise photon. The degree of indistinguishability is parametrized by the probability p that the fully depolarized photon E is completely indistinguishable from the photon E .

In order to maximize the degree of indistinguishability between the photon of modes k_B and k_E mixed on the beam splitter BS we adopt narrower interference filters and single mode fibers on the output modes. Hence we insert interference filters on mode $k_{B'}$ and $k_{E'}$, with $\Delta\lambda = 1.5nm$. Referring to the previous nomenclature, the density matrix τ can be written as: $\tau_{AB} = p\sigma_{coh} + (1 - p)\rho_{inc}$. As first step, we have estimated the degree of indistinguishability between the photon belonging to mode k_B and the one associated to k_E . This measurement has

been carried out by realizing an Hong-Ou-Mandel interferometer [106] adopting a balanced 50 : 50 beam splitter instead of BS . The photons on modes $k_{B'}$ and $k_{E'}$ are measured in the same polarization state $|H\rangle$. The visibility of the Hong-Ou-Mandel dip has been measured to be $V = (0.67 \pm 0.02)$. By subtracting estimated double pairs contributions to the three-photon coincidence we have obtained a value of the visibility (0.75 ± 0.02) . We attribute the mismatch with the unit value to a different spectral profile between the coherent beam and the fluorescence, which induces a distinguishability between photons on the input modes of the beam splitter. From the visibility of the dip, we estimate a value of p equal to (0.85 ± 0.05) . Hence we have checked the Hong-Ou-Mandel interference with the unbalanced beam splitter BS , and we have obtained a visibility of (0.40 ± 0.02) . This result has been compared to a theoretical visibility V previously calculated considering the expression $V = p2RT/(R^2 + T^2) = (0.62 \pm 0.05)$ with p as indicated by the Hong-Ou-Mandel experiment, and $T = 0.3$. To carry out the experiment the optical delay has been set in the position $\Delta t = 0$. The mismatch between the two visibilities are due to multi-photon contributions. Indeed by taking into account the accidental coincidence we have estimated $V = (0.49 \pm 0.03)$.

I) Mixing.

Analogously to what has been showed in the distinguishable case, after the mixing on the BS , once there is one photon per output mode, the input state evolves into a noisy state represented by the density matrix $\tilde{\tau}^I$. The experimental density matrix is characterized by a fidelity with theory : $F(\tilde{\tau}^I, \tau^I) = (0.86 \pm 0.02)$ and vanishing concurrence ($\tilde{C}_I = 0$).

II) Measurement.

After measuring the photon on mode $k_{E'}$, the density matrix $\tilde{\tau}^I$ evolves into $\tilde{\tau}^{II}$: FIG.(5.10-II). The entanglement is localized with a concurrence equal to $\tilde{C}_{II} = (0.15 \pm 0.03) > 0$ to be compared with $C_{II} = 0.22$; in this case the probability of success reads $\tilde{P}_{II} = (0.22 \pm 0.01)$, while theoretically we expect $P_{II} = 0.2$. The fidelity with the theoretical state is $F(\tilde{\tau}^{II}, \tau^{II}) = (0.96 \pm 0.01)$.

III) Filtration.

Applying experimentally the filtration with the parameters $A_A = 0.12$, and $A_B = 0.30$ we obtain the state shown in FIG.(5.10-III). Hence we measure a higher concurrence $\tilde{C}_{III} = (0.50 \pm 0.10) > \tilde{C}_{II}$ while the expected theoretical value is $C_{III} = 0.47$. The filtered state has $F(\tilde{\tau}^{III}, \tau^{III}) = (0.92 \pm 0.04)$, and is post-selected with an overall success rate equal to $P_{total} = \tilde{P}_{III}\tilde{P}_{II} = (0.10 \pm 0.01)$, where theoretically $P_{III}P_{II} = 0.09$. This is a clear experimental demonstration of how an induced indistinguishability enhances the localized concurrence.

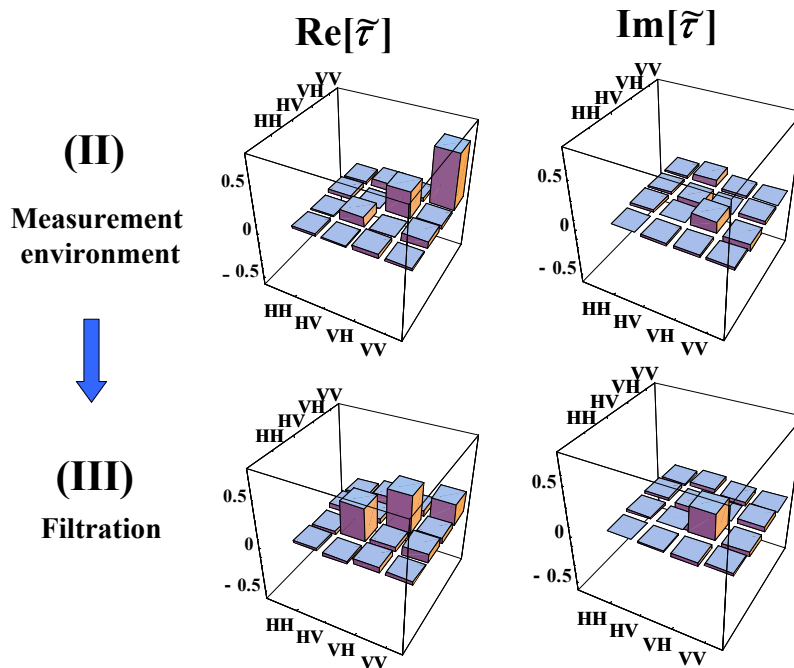


Figure 5.10: Experimental density matrix for partially indistinguishable photons: $\tilde{\tau}$ with $p = 0.85$. **II)** $\tilde{\tau}^{II}$, **III)** $\tilde{\tau}^{III}$.

5.4 Appendix

In this appendix we give an extension of the above theoretical result for any linear coupling on the beam splitter.

To describe a linear coupling (beam splitter) with different transmissivity for vertical and horizontal polarization, we use the amplitude transmissivities t_v and t_h . The intensity transmissivities are then $T_V = t_v^2$ and $T_H = t_h^2$ and the previous result can be obtained taking $T = T_V = T_H$.

5.4.1 Coherent coupling

After the mixing of coherent (indistinguishable) photons B and E on the beam splitter, without any access to the photon E , the single state transforms to the mixed state (if two photons leave separately) exhibiting the concurrence

$$C_{coh}^I = \max \left(0, \frac{2t_v t_h |t_h^2 - 1 + t_v^2| - (1 - t_v^2)(1 - t_h^2)}{2P_{coh}^I} \right), \quad (5.46)$$

where $P_{coh}^I = (2t_v^2 t_h^2 + (1 - 2t_v^2)^2 + (1 - 2t_h^2)^2 + 2(1 - t_v^2)(1 - t_h^2))/4$ is the success probability. The concurrence is depicted on FIG. 5.11, there is evidently a large area where the concurrence vanishes completely and the entanglement is lost between A and B .

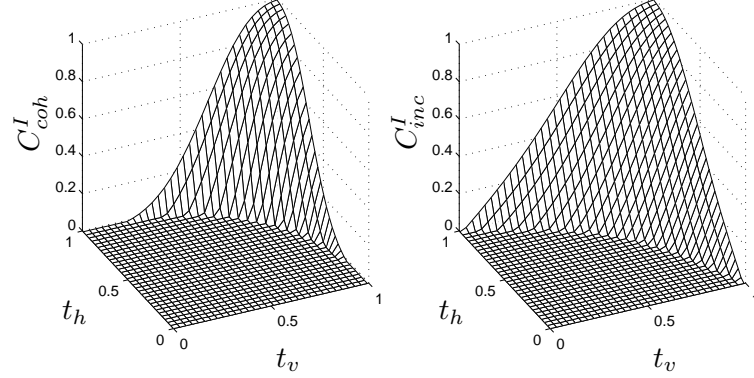


Figure 5.11: Concurrence before the measurement for coherent (left) and incoherent (right) couplings.

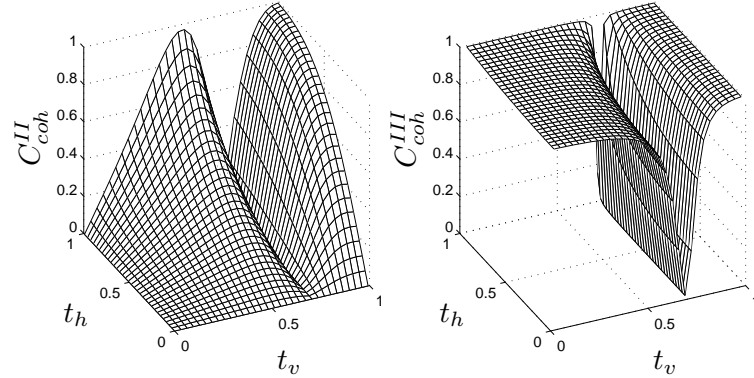


Figure 5.12: Concurrence after the measurement (left) and after the filtration with $\epsilon = 0.1$ (right) for indistinguishable photons (coherent coupling).

To restore the entanglement a general projection measurement can be considered on the photon E . But it is too complex to find an optimal projection analytically, rather the optimal measurement can be found numerically, for the particular values of t_v and t_h . On the other hand, it is possible to find a sufficient condition to restore the entanglement for some particular orientation of the measurement. Let us assume the projection of the photon E on the state $|V\rangle$. Then the state σ_{coh} changes and exhibits the concurrence

$$C_{coh}^{II} = \frac{t_h t_v |1 - 2t_v^2|}{2P_{coh}^{II}}, \quad (5.47)$$

where $P_{coh}^{II} = (t_v^2 t_h^2 + (1 - 2t_v^2)^2 + (1 - t_v^2)(1 - t_h^2))/4$ is the success rate. Such state is always entangled except $t_h = 0$ or $t_v^2 = 1/2, 0$ and can be further filtered out by

the filter F1 on photon B which makes $|V\rangle \rightarrow \frac{2t_v^2-1}{t_v t_h} |V\rangle$ for $t_h > \frac{|2t_v^2-1|}{t_v}$ or by the filter F1 on photon A $|H\rangle \rightarrow \frac{t_v t_h}{2t_v^2-1} |H\rangle$ for $t_h < \frac{|2t_v^2-1|}{t_v}$ and subsequently, the filter F2 attenuating horizontal polarization $|H\rangle \rightarrow \sqrt{\epsilon} |H\rangle$, applied to both photons A and B. As result, the state is transformed by both types of filtering to a new state with the corresponding concurrence

$$C_{coh}^{III}(\epsilon) = \frac{\epsilon(1-2t_v^2)^2}{2P_{coh_1}^{III}} = \frac{\epsilon t_v^2 t_h^2}{2P_{coh_2}^{III}}, \quad (5.48)$$

where $P_{coh_1}^{III} = (2\epsilon(1-2t_v^2)^2 + \epsilon^2(1-t_v^2)(1-t_h^2))/4$ is the success rate of the localization using the first type of filtration F1 on photon B and $P_{coh_2}^{III} = (2\epsilon(t_v t_h)^2 + \epsilon^2(1-t_v^2)(1-t_h^2)/(1-2t_v^2)^2)/4$ is the success rate of the restoration using the second type of filtration on photon A. The concurrence approaches unity as $\epsilon \rightarrow 0$. The similar results can be obtained for the projection of the photon E on the state $|H\rangle$, only the substitution $t_h \leftrightarrow t_v$ is necessary. In conclusion, except the cases $t_v^2, t_h^2 = 1/2$, the entanglement can be always localized and enhanced arbitrarily close to maximal pure entangled state, at cost of the success rate, similarly to previous analysis. The concurrences after the measurement and the one after the filtration in the localization procedure are depicted on FIG. 5.12.

5.4.2 Incoherent coupling

For the incoherent (distinguishable) photons, without any access to the photon E , after the mixing at the beam splitter the singlet state transforms to a state exhibiting the concurrence

$$C_{inc}^I = \max \left(0, \frac{t_h t_v (t_h^2 + t_v^2) - (1-t_v^2)(1-t_h^2)}{2P_{inc}^I} \right), \quad (5.49)$$

where $P_{inc}^I = (2(1-t_v^2)(1-t_h^2) + (1-t_h^2)^2 + t_h^2(t_h^2 + t_v^2) + (1-t_v^2)^2 + t_v^2(t_h^2 + t_v^2))/4$ is the probability of success. Similarly, there is a large area of the parameters in which the concurrence vanishes and the entanglement is lost between A and B , as can be seen from FIG. 5.11.

Similarly, it is sufficient to localize entanglement by the projection of the environmental photon on the state $|V\rangle$. After the successful projection, the mixed state has concurrence

$$C_{inc}^{II} = \frac{t_h t_v^3}{2P_{inc}^{II}}, \quad (5.50)$$

where $P_{inc}^{II} = (t_h^2 t_v^2 + t_v^4 + (1-t_v^2)^2 + (1-t_v^2)(1-t_h^2))/4$ is the success rate of the projection. Except trivial $t_v, t_h = 0$, the entanglement is always localized by the

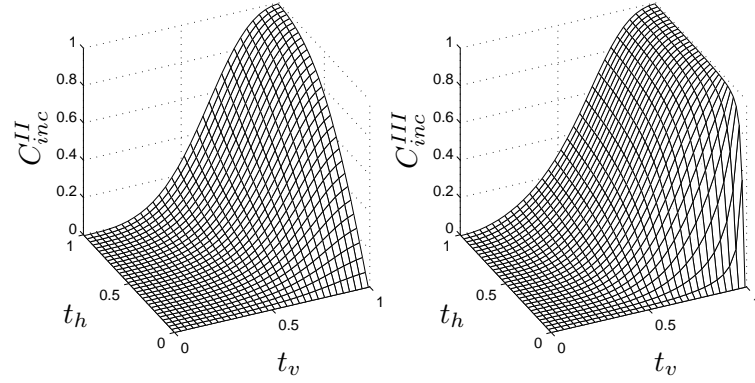


Figure 5.13: Concurrence after the measurement (left) and after the filtration with $\epsilon = 0.1$ (right) for incoherent coupling.

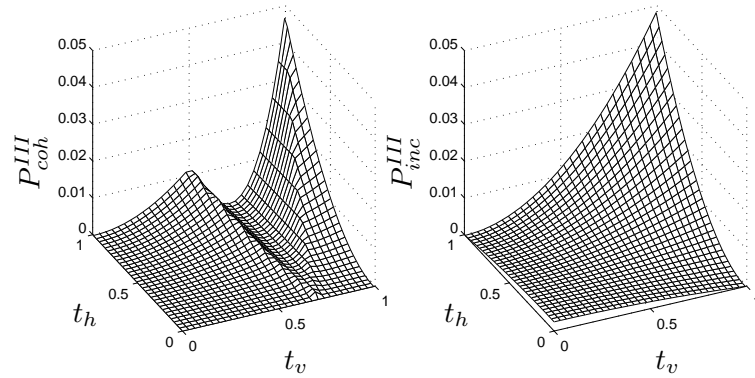


Figure 5.14: Success rate after the filtration with $\epsilon = 0.1$ for indistinguishable photons (left) and distinguishable photons (right)

projection on the environment. But for this case, optimal filtration by F1 and F2 defined as $|V\rangle \rightarrow \frac{t_v t_h}{\sqrt{t_v^4 + (1-t_v^2)^2}}|V\rangle$ and $|H\rangle \rightarrow \sqrt{\epsilon}|H\rangle$ produces the state with overall probability of success $P_{inc}^{III} = (2\epsilon t_v^2 t_h^2 + \epsilon^2(1-t_v^2)(1-t_h^2))/4$, which gives the concurrence

$$C_{inc}^{III}(\epsilon) = \frac{\epsilon t_v^4 t_h^2}{2P_{inc}^{III} \sqrt{t_v^4 + (1-t_v^2)^2}} \quad (5.51)$$

In the limit $\epsilon \rightarrow 0$ it gives the maximal concurrence

$$C_{inc}^{III} = \frac{t_v^2}{\sqrt{t_v^4 + (1-t_v^2)^2}}. \quad (5.52)$$

In a similar way as in the symmetrical case, the maximal entanglement cannot be approached if the photon E is in principle distinguishable. The concurrence before and after the filtration is depicted on FIG. 5.13. Success rates after the filtration for both the indistinguishable and distinguishable photons are plotted in FIG. 5.14.

5.5 Conclusion

We have shown that two-qubit entanglement lost during coupling of the one qubit from the pair with another “environmental” qubit may be recovered back by localization protocol. The recovery procedure, entanglement localization, uses the fact that entanglement is redistributed among all the parties involved including the environment. Proper single-copy quantum measurement on the environment together with feed-forward correction on the outgoing states localizes with some probability of success the entanglement back to the original parties. We have analyzed the single-copy localization protocol for three photons involving general linear coupling among the photons and arbitrary coherence between coupled photons. In the coherent coupling scenario the entanglement may be localized asymptotically to one ebit (maximal entanglement between two qubits e.g. possessed by singlet). In the incoherent or partially coherent regime we found that the entanglement cannot approach the maximal entanglement however we can still get non-zero entanglement and by proper single-copy distillation also a state violating Bell inequality. We have proposed an experimental setup for verification of our theoretical predictions. The experiment using single photons encoded in polarizations was performed that verified our theoretical predictions.

All our results on the quantum localization together with experimental implementation were published here:

- **M. Gavenda, R. Filip, E. Nagali, F. Sciarrino, and F. De Martini,** *Complete analysis of measurement-induced entanglement localization on a three-photon system*, Phys. Rev. A 81, 022313 (2010).
- **E. Nagali, F. Sciarrino, F. De Martini, M. Gavenda, and R. Filip,** *Entanglement concentration after a multi-interactions channel*, Adv. Sci. Lett. 2, 448-454 (2009).
- **F. Sciarrino, E. Nagali, F. De Martini, M. Gavenda, and R. Filip,** *Entanglement localization after coupling to an incoherent noisy system*, Phys. Rev. A 79, 060304 (2009).

Chapter 6

Particle distinguishability and decoherence

In this chapter, we investigate how distinguishability of a “noise” particle degrades interference of the “signal” particle. The signal, represented by an equatorial state of a photonic qubit, is mixed with noise, represented by another photonic qubit, via linear coupling on the beam splitter. We show the degradation of the “signal” photon interference depending on the degree of indistinguishability between “signal” and “noise” photon. When the photons are principally completely distinguishable but technically indistinguishable the visibility drops to the value $1/\sqrt{2}$. As the photons become more indistinguishable the maximal visibility increases and reaches the unit value for completely indistinguishable photons. We have examined this effect experimentally using setup with fiber optics two-photon Mach-Zehnder interferometer.

6.1 Theoretical framework

The simplest system in quantum information is a qubit. In many applications and experiments (like in quantum key distribution, tests of Bell inequalities, etc.) only a subset of all possible states of a qubit is used. Namely, the set of equatorial states (they lie on the equator of the Bloch sphere) represented by a coherent superposition

$$\frac{1}{\sqrt{2}} (|0\rangle + \exp(i\varphi) |1\rangle) \quad (6.1)$$

of two basis states $|0\rangle$ and $|1\rangle$. Phase φ is used to encode information. We investigate how noise can affect the coherence of equatorial state of qubit. We suppose no fluctuation of phase and no interaction with the environment (therefore no entanglement can appear between the qubit and the environment). Let us repre-

sent our qubit by a single particle distributed between two modes A and B . Its equatorial state can be described as

$$|\Psi\rangle_{AB} = \frac{1}{\sqrt{2}} (|1, 0\rangle_{AB} + \exp(i\varphi) |0, 1\rangle_{AB}), \quad (6.2)$$

where 0 and 1 represent the number of particles. The noise is caused by another particle in mode B' which can be confused with the original particle. We suppose that modes B and B' are *principally* distinguishable but *technically* indistinguishable. It means our detectors cannot discriminate them. We will consider the situation when a “noise” particle is created in mode B' and subsequently one particle is annihilated either from mode B or B' (our device cannot distinguish between them).

To examine this situation experimentally, we use a Mach-Zehnder (MZ) interferometer and a source of photon pairs (Fig. 6.1). The “noise” photon with variable distinguishability from the “signal” one is fed into one arm of the interferometer. If the “noise” particle was created in mode B it would be *principally indistinguishable* from the “signal” particle in mode B . For a bosonic field the total quantum state after the creation process $a_B^\dagger |\Psi\rangle_{AB}$ reads

$$|\Psi'\rangle_{AB} = \frac{1}{\sqrt{3}} (|1, 1\rangle_{AB} + \sqrt{2} \exp(i\varphi) |0, 2\rangle_{AB}). \quad (6.3)$$

It has full coherence: the phase information is fully preserved. The indistinguishable photon can be eliminated by the act of annihilation $a_B |\Psi'\rangle_{AB}$ ending up with state

$$|\Psi''\rangle_{AB} = \frac{1}{\sqrt{5}} (|1, 0\rangle_{AB} + 2 \exp(i\varphi) |0, 1\rangle_{AB}). \quad (6.4)$$

It can be further probabilistically converted to the original state of the signal qubit applying attenuation $\eta_B = 1/4$ in mode B . Since the both particles are indistinguishable, it does not matter which one has been actually taken out. The visibility of interference can reach unity again. We define the single photon visibility by the standard formula

$$V = \frac{P_{\max} - P_{\min}}{P_{\max} + P_{\min}}, \quad (6.5)$$

where $P_{\max} = \max_{\varphi} P(\varphi)$, $P_{\min} = \min_{\varphi} P(\varphi)$ with $P(\varphi)$ being the probability to detect photon at detector D depending on phase φ .

If the “noise” particle is *principally distinguishable* from the “signal” one, it can be described by creation operation $a_{B'}^\dagger |\Psi\rangle_{AB} |0\rangle_{B'}$. In principle, it could be filtered out, because it differs in its properties from the “signal” particle. But,

quite typically, our filters are not selective enough to enable it. If the disturbing particle is only *technically indistinguishable*, the total state of the system is transformed to

$$|\Phi'\rangle = \frac{1}{\sqrt{2}}(|1, 0, 1\rangle_{ABB'} + \exp(i\varphi) |0, 1, 1\rangle_{ABB'}) \quad (6.6)$$

after the creation in mode B' . Because we are not able to discriminate modes B and B' , to remove a single particle we just randomly annihilate a single particle either from B or B' (with no prior knowledge this strategy is fully symmetrical). Further, without any access to mode A , this process can be described by two “subtraction” operators: $S_1 = a_B \otimes 1_{B'}$ and $S_2 = 1_B \otimes a_{B'}$ acting with equal probabilities. Applying these operators on $\rho' = |\Phi'\rangle\langle\Phi'|$, i.e. $S_1\rho'S_1^\dagger + S_2\rho'S_2^\dagger$, one gets the resulting mixed state

$$\rho'' = \frac{2}{3}|\Psi\rangle_{AB}\langle\Psi| \otimes |0\rangle_{B'}\langle 0| + \frac{1}{3}|00\rangle_{AB}\langle 00| \otimes |1\rangle_{B'}\langle 1|. \quad (6.7)$$

Because our detectors cannot distinguish whether the particle came from mode B or B' , the visibility of interference is now $V'' = 2/3$. It can be probabilistically enhanced by a proper attenuation $\eta_B = \eta_{B'}$ in modes B and B' . This transforms the total state to

$$\begin{aligned} \rho''' = & \frac{1}{2\eta_B} [|100\rangle\langle 100| + \eta_B |010\rangle\langle 010| + \eta_B |001\rangle\langle 001| \\ & + \sqrt{\eta_B} (e^{i\varphi} |010\rangle\langle 100| + e^{-i\varphi} |100\rangle\langle 010|)]. \end{aligned} \quad (6.8)$$

Clearly, if $\eta_B = 1/2$ one balances the probability of having a particle in mode A with the probability of having it either in mode B or B' . Then the visibility is maximal and reaches the value

$$V_{dis} = \frac{1}{\sqrt{2}}. \quad (6.9)$$

In comparison to the previous case of indistinguishable particles, this reduction of visibility represents a fundamental impact of the principal distinguishability of the “signal” and “noise” particles. The loss of coherence is a result of an elementary ignorance of our measurement apparatus. There is a difference between our result and the one reported in [107], where visibility completely vanishes for distinguishable photons. According to Englert’s inequality $V^2 + K^2 \leq 1$ [108, 109], this elementary visibility reduction corresponds to overall which-way knowledge $K < 1/\sqrt{2}$ accessible in the experiment.

If N completely distinguishable particles are created simultaneously in modes associate to mode B and, subsequently, N particles are simultaneously annihilated in these modes and mode B , visibility rapidly decreases with increasing N :

$$V_{dis}(N) = \frac{1}{\sqrt{N+1}}. \quad (6.10)$$

On the other hand if the particles are created and annihilated subsequently, i.e. after any single-particle creation a single particle is always annihilated, visibility is decreasing even faster:

$$V_{dis}(N) = \left(\frac{1}{\sqrt{2}}\right)^N. \quad (6.11)$$

In the experiment, mode A is represented by the upper arm of the interferometer (Fig. 6.1) and modes B, B' by the lower arm (they are distinguishable in time domain). Creation and annihilation process is emulated by a beam splitter. The action of the beam splitter can be described by a unitary operator $U = \exp[\theta(a^\dagger a_{aux} - a_{aux}^\dagger a)]$, where “aux” denotes the auxiliary mode and θ is related to the intensity transmittance by the formula $T = \cos^2 \theta$. If $|\theta| \ll 1$ and there is a proper state in the auxiliary mode, U well approximates action of creation, a^\dagger , or annihilation, a , operators. The coincidence measurement guaranties that only those situations are taken into account, when exactly one photon is annihilated and one photon is detected at the output of the interferometer.

To be realistic and comparable with experimental results, the theoretical prediction must take into account a finite coupling (i.e. transmittances and reflectances of beam splitters) as well as all insertion losses.

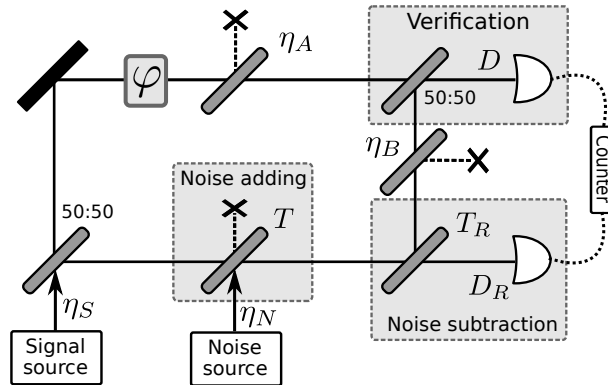


Figure 6.1: The simple scheme of Mach-Zehnder two-photon interferometer illustrates the process of interference measurement.

In Fig. 6.1 the signal source generates single photons which are coupled, with efficiency η_S , to the interferometer and afterwards they are split equally likely to the upper or lower arm of the interferometer. In the upper arm we can set the

phase shift φ and adjust losses by a beam splitter with transmissivity η_A (to achieve maximum interference). The noise source feeds single photons into the lower arm of the interferometer with coupling efficiency η_N and then the photons are coupled by a beam splitter with transmissivity T to the signal photons. The internal losses of the interferometer are modelled by a beam splitter with transmissivity η_B . As was indicated in the introduction, in order to subtract noise we suggested to annihilate one photon from the lower arm of the interferometer. This is accomplished by inserting another beam splitter which transmits photons with ratio T_R to another detector D_R . To evaluate the effect of the noise subtraction we measure visibility of the signal from detector D conditioned on the detection event from the detector D_R . Calculation for fully indistinguishable “noise” photon leads to visibility

$$V_{ind} = \frac{4\sqrt{\eta_A\eta_B T(1-T_R)}}{\eta_A + 4\eta_B T(1-T_R)}. \quad (6.12)$$

Optimizing the values of free parameters we can reach

$$V_{ind}^{max} = 1 \quad (6.13)$$

for $\eta_A = \eta_B T$, $T_R = 3/4$. The perfect visibility is achieved, as was predicted also in the previous discussion of simplified model. In the fully distinguishable scenario the visibility reads

$$V_{dis} = \frac{2\sqrt{\eta_A\eta_B T(1-T_R)}}{\eta_A + 2\eta_B T(1-T_R)}. \quad (6.14)$$

If we optimize the values of free parameters we can reach

$$V_{dis}^{max} = \frac{1}{\sqrt{2}} \quad (6.15)$$

for $\eta_A = \eta_B T$, $T_R = 1/2$. We can see the drop in visibility to the value $1/\sqrt{2}$.

In practice, the photons are partially indistinguishable. We can describe this situation as a mixture of the two limit cases: With probability p the “signal” and “noise” photons are principally indistinguishable, otherwise they are principally distinguishable! We have repeated the calculation of visibility (similarly to the previous extreme cases) for the above defined mixture of an indistinguishable and distinguishable “noise” photon. The visibility reads

$$V(p) = \frac{2(1+p)\sqrt{\eta_A\eta_B T(1-T_R)}}{\eta_A + 2(1+p)\eta_B T(1-T_R)}. \quad (6.16)$$

Optimizing the values of free parameters the visibility reaches its maximum

$$V^{max}(p) = \sqrt{\frac{1+p}{2}}, \quad (6.17)$$

for $\eta_A = \eta_B T$, $T_R = (1 + 2p)/[2(1 + p)]$. The more distinguishable is the noise photon from the signal photon the lower visibility we can obtain. The transmissivity T , determining the strength of the coupling between the noise and signal photon, has no influence on the visibility.

6.2 Experimental implementation

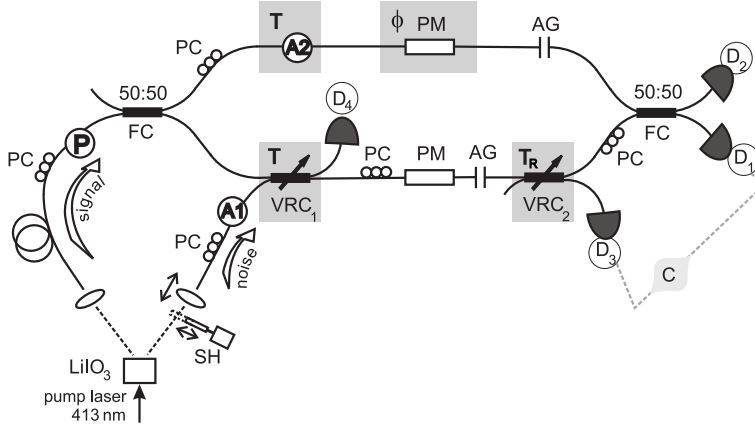


Figure 6.2: Experimental setup. Shutter (SH), polarization controller (PC), polarizer (P), attenuator (A), phase modulator (PM), adjustable air-gap (AG), fiber coupler (FC), variable-ratio coupler (VRC), detector (D).

We have used a setup depicted in Fig. 6.2 to experimentally test the theoretically predicted visibility (6.17) for the two extreme cases of distinguishability. The key part of the setup is the MZ interferometer build of fiber optics that allows us to simply control transmissivities T and T_R via variable-ratio couplers (VRCs) within the range 0-100%. Signal and noise photons are created by type-I degenerate spontaneous parametric down-conversion in a nonlinear crystal of LiIO_3 pumped by a cw Kr-ion laser (413 nm). Photons from each pair are tightly time correlated, have the same polarization and the same spectrum centered at 826 nm. The degree of distinguishability of signal and noise photons can be tuned changing the time delay between their wave-packets at VRC_1 . This is realized moving a motorized translation stage connected to the fiber coupling system at the “noise” side. All other characteristics of the photons are identical.

Before the measurement the source of photon pairs is adjusted by optimizing the visibility of two-photon interference at VRC₁ with splitting ratio 50:50. The visibility of Hong-Ou-Mandel (HOM) dip [106] reaches typically values about 98%. Then the equality of intensities of signal and noise coupled to the fibers is verified measuring the count rates at detectors D₃ and D₄. The count rates of the noise photons at these detectors have to be double in comparison with the count rates of the signal photons. The required signal to noise ratio is then set tuning the intensity transmissivity T of VRC₁. According to the theoretical proposal, the transmissivity of the upper arm of the MZ interferometer is also set to the value T using attenuator A2. At this point we unbalance the interferometer setting the optimal transmissivity T_R of VRC₂. This variable ratio coupler separates a part of the light from the lower interferometer arm for a post-selection measurement on the detector D₃. It should be stressed that these additional losses are not compensated in the upper arm of the MZ interferometer.

Technical remarks:

- (i) To accomplish proposed experiment, only one phase modulator in the upper arm of the MZ interferometer is needed. The second phase modulator in the lower arm just guarantees the same dispersion in both interferometer arms. This trick allowed to increase the visibility approximately by 13 % to 94%.
- (ii) All used detectors are Perkin-Elmer single-photon counting modules. To implement the post-selection measurement the signals from detectors are processed by coincidence electronics with a coincidence window of 2 ns.
- (iii) The absolute phase in optical fibers is influenced by temperature changes. Resulting undesirable phase drift is reduced by a thermal isolation of MZ interferometer and the residual phase drift is compensated by an active stabilization.

6.3 Results

The aim of the experiment is to show how the visibility of the signal photon is affected by a distinguishable and indistinguishable “noise” photon after the “noise subtraction”. We measured coincidence rate C between detectors D₁ and D₃. Intensity transmissivity of VRC₂ was adjusted so that the visibility of coincidence rate C was maximal, i.e., $T_R = 1/2$ for distinguishable photons and $T_R = 3/4$ for indistinguishable photons. The visibility of C was measured for different values of the transmissivity T . $T = 100\%$ represents no added noise case, $T = 0\%$ means that the signal photon can not pass through the lower arm of the MZ interferometer. These two limit cases could not be measured, because the

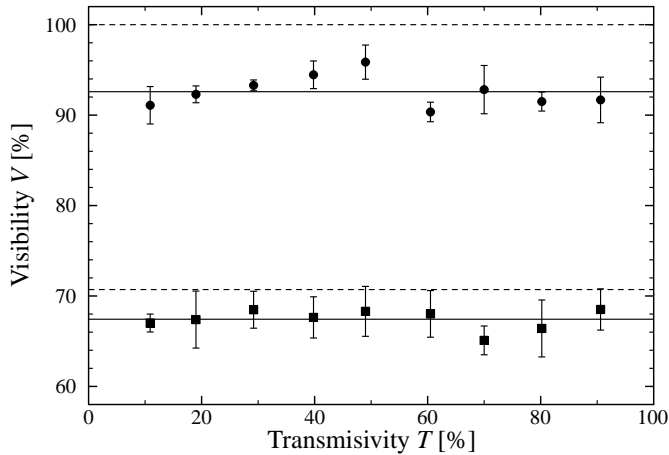


Figure 6.3: Visibility V as a function of the transmissivity T . Symbols denote experimental results; squares correspond to the case of distinguishable photons and circles to the case of indistinguishable photons. Solid lines are fits of measured data and dashed lines are theoretical predictions.

coincidence rate C vanishes.

Figure 6.3 shows visibilities of the coincidence-rate interference patterns. Each interference-fringe measurement, consisting of 41 phase-steps, was repeated five times. Coincidence-rate measurement for each phase step takes typically 3 s. After each three-second measurement period the phase was actively stabilized. The results displayed in Fig. 6.3 support the theoretical prediction that visibility V does not depend on T . Obtained mean value of visibility is $67.4 \pm 1.1\%$ for distinguishable noise photons (the theoretical value is $1/\sqrt{2} \approx 70.7\%$) and $92.6 \pm 1.7\%$ for indistinguishable noise photons (the theoretical value is 100%). Shown error bars represent statistical errors. Systematic shifts of the values are due to experimental imperfections. It should be noted that the measurement with distinguishable noise photons is more robust. In the case of indistinguishable photons the visibility is very sensitive to fluctuations of the time overlap of the two photons. Due to this fact, the visibility measured with distinguishable photons lies closer to the theoretical limit.

6.4 Conclusion

We have investigated a decoherence model based on a mixing of particle representing a system with another particle representing noise. The particles are in principle distinguishable during the mixing stage and become technically indistinguishable when subject to verification of its interference state. The interference

of the signal particle is lowered by discrete amount depending on the number of noise particle involved. While the usual decoherence processes behaves continuously in time we have obtained discrete model of decoherence process. We have proposed an experimental setup for verification of our theoretical predictions. The experiment based on two-photon Mach-Zehnder interferometer was performed and verified our theoretical results. The theoretical results together with the experimental implementation were published here:

- **M. Gavenda, L. Čelechovská, J. Soubusta, M. Dušek, R. Filip**
Visibility bound caused by a distinguishable noise particle, Phys. Rev. A 83, 042320 (2011).

Chapter 7

Summary and Outlook

In chapter 4 a single-copy quantum adaptation of channels has been proposed to stop non-trivial sudden death of entanglement arising in a composite of the independent channels. The adaptation differs from the entanglement distillation, it rather prepares the entangled states for the transmission through the subsequent channel. A power of both the unitary operation and quantum filters to completely reduce the sudden death of entanglement has been demonstrated. The presented results have direct application for the quantum key distribution through noisy channel and, in an extended multi-qubit version, also for the preparation of cluster states for quantum computing. The protocol is further analyzed and an experimental verification is under preparation.

In the chapter 5 we have discussed the role of the coherence in an elementary polarization entanglement three-photon localization protocol, both theoretically and experimentally, especially for the cases of complete redirection of the entanglement to an unpolarized surrounding photon. Theoretically, a full coherence (indistinguishability) of noisy surrounding photon and one photon from the maximally entangled state of two photons is a necessary condition for perfect entanglement localization. Moreover, also for the partially coherent or even fully incoherent photon the localization protocol is still able to restore non-zero entanglement. Using local single-copy polarization filters, the entanglement can be enhanced even to violate the Bell inequalities. The generalization of the results to linear polarization sensitive coupling is also enclosed. Experimentally, the localization of entanglement is demonstrated for both fully incoherent as well as for the highly (but still partially) coherent coupling. The restoration of entanglement after its previous redirection to the surrounding systems was experimentally verified, also the positive role of the coherence induced by the spectral filters has been experimentally checked. These results clearly show the broad applicability of the basic element of the polarization-entanglement localization protocol in realis-

tic situations, where the surrounding uncontrollable noisy system exhibiting just moderate coherence completely destroys the entanglement due to the coupling process. In these cases, the collective entanglement distillation method without a measurement on the surrounding system can not restore any entanglement out of the coupling. An open question is whether after such multiple decoherence events on both sides of the entangled state, non-zero entanglement can be as well always localized back just by local measurements and classical communication, or a collective localization measurement will be required. Further, an extension from fixed number of surrounding particles to randomly fluctuating number of the surrounding particles will be interesting. Another interesting direction is to analyze the entanglement localization after another kind of the partially coherent coupling, especially between atoms/ions and light or between individual atoms or ions. This gradual investigation will give a final answer to an important physical question: how to manipulate quantum entanglement distributed by the coupling to noisy incoherent complex environments. Further investigations may involve multipartite states of environment. Entanglement localization in such a complex environment will demand the usage of numerical methods to find an optimal solution.

We have observed in the chapter 6 how the noise represented by an additional distinguishable particle can degrade interference. It is known that as a consequence of decoherence events very fast sudden death of entanglement can happen and Bell-inequality violation can disappear [46]. So, let us imagine now that instead of a single signal photon entering the interferometer through the input beam splitter we have a photon inside the interferometer which is a member of a pair maximally entangled in spatial modes. So we have two maximally entangled qubits, one of them goes through our noisy “channel” followed by the “noise subtraction” and finally it is measured in the basis consisting of two orthogonal equatorial states. Pairs of maximally entangled qubits can be used to test the exclusivity of quantum mechanics. If they are measured locally in proper bases (which can be fully constructed from the equatorial states) the results violate Bell (or CHSH) inequalities [5]. However, once one of the qubits is sent through our channel and once the detectors are not able to distinguish between modes B and B' no violation of the Bell inequality is observed. To reveal the violation, a measurement outside the equatorial plane has to be performed. It is not surprising, since the considered decoherence process is basis dependent. It fully disturbs only the results of measurements in the equatorial plane. Tittel et al. [110] used energy-time entangled photons to test Bell-inequality violation under the dephasing process in an optical fiber and they have proved that the necessary condition

to observe the violation reads $V > 1/\sqrt{2}$. In the decoherence process described above the maximal visibility (in the case of “distinguishable” noise) reaches just this boundary value. We are now working on an experimental proposal testing the situation with the violation of Bell inequalities in the decoherence process described above.

References

- [1] Nielsen, M. A. and Chuang, I. L. Quantum Computation and Quantum Information, Cambridge University Press, Cambridge, (2000).
- [2] Schrödinger, E. *Naturwissenschaften* **23**, 807 (1935).
- [3] Einstein, A., Podolsky, B., and Rosen, N. *Phys. Rev.* **47**, 777 (1935).
- [4] Bell, J. S. *Physics* **1**, 195 (1964).
- [5] Clauser, J. F., Horne, M. A., Shimony, A., and Holt, R. A. *Phys. Rev. Lett.* **23**, 880 (1969).
- [6] Aspect, A., Dalibard, J., and Roger, G. *Phys. Rev. Lett.* **49**, 1804 (1982).
- [7] Kwiat, P. G., Mattle, K., Weinfurter, H., and Zeilinger, A. *Phys. Rev. Lett.* **75**, 4337 (1995).
- [8] Weihs, G., Jennewein, T., Simon, C., Weinfurter, H., and Zeilinger, A. *Phys. Rev. Lett.* **81**, 5039 (1998).
- [9] Raussendorf, R. and Briegel, H. J. *Phys. Rev. Lett.* **86**, 5188 (2001).
- [10] Curty, M., Lewenstein, M., and Lütkenhaus, N. *Phys. Rev. Lett.* **92**, 217903 (2004).
- [11] Ekert, A. *Phys. Rev. Lett.* **67**, 661 (1991).
- [12] Bennet, C. H., Brassard, G., Crepeau, C., Jozsa, R., Peres, A., and Wootters, W. K. *Phys. Rev. Lett.* **70**, 1895 (1993).
- [13] Bennet, C. H. and Wiesner, S. J. *Phys. Rev. Lett.* **69**, 2881 (1992).
- [14] Bouwmeester, D., Pan, J.-W., Mattle, K., Eibl, M., Weinfurter, H., and Zeilinger, A. *Nature* **390**, 575 (1997).
- [15] Jennewein, T., Simon, C., Weihs, G., Weinfurter, H., and Zeilinger, A. *Phys. Rev. Lett.* **84**, 4729 (2000).
- [16] Mattle, K., Weinfurter, H., Kwiat, P. G., and Zeilinger, A. *Phys. Rev. Lett.* **76**, 4656 (1996).
- [17] Furusawa, A., Sørensen, J. L., Braunstein, S. L., Fuchs, C. A., Kimble, H. J., and Polzik, E. S. *Science* **282**, 706 (1998).

- [18] <http://www.magiqtech.com>.
- [19] <http://www.idquantique.com>.
- [20] Brukner, C., Zukowski, M., Pan, J.-W., and Zeilinger, A. *Phys. Rev. Lett.* **92**, 127901 (2004).
- [21] Venzl, H. and Freyberger, M. *Phys. Rev. A* **75**, 042322 (2007).
- [22] Giovannetti, V., Lloyd, S., and Maccone, L. *Science* **306**, 1330 (2004).
- [23] Jozsa, R., Abrams, D. S., Dowling, J. P., and Williams, C. P. *Phys. Rev. Lett.* **85**, 2010 (2000).
- [24] Zurek, W. H. *Rev. Mod. Phys.* **75**, 715 (2003).
- [25] Schlosshauer, M. *Rev. Mod. Phys.* **76**, 1267 (2004).
- [26] Wootters, W. K. and Zurek, W. H. *Phys. Rev. D* **19**, 473 (1979).
- [27] Zurek, W. H. *Phys. Rev. D* **26**, 1862 (1982).
- [28] Joos, E. and Zeh, H. D. *Z. Phys. B* **59**, 223 (1985).
- [29] Brune, M., Hagley, E., Dreyer, J., Maître, X., Maali, A., Wunderlich, C., Raimond, J. M., and Haroche, S. *Phys. Rev. Lett.* **77**, 4887 (1996).
- [30] T. Pfau, S. S., Kurtsiefer, C., Ekstrom, C. R., and Mlynek, J. *Phys. Rev. Lett.* **73**, 1223 (1994).
- [31] Chapman, M. S., Hammond, T. D., Lenef, A., Schmiedmayer, J., Rubenstein, R. A., Smith, E., and Pritchard, D. E. *Phys. Rev. Lett.* **75**, 3783 (1995).
- [32] Gavenda, M., Čelechovská, L., Soubusta, J., Dušek, M., and Filip, R. *Phys. Rev. A* **83**, 042320 (2011).
- [33] Palma, G. M., Suominen, K.-A., and Ekert, A. K. *Proc. Roy. Soc. London Ser. A* (1996).
- [34] Lidar, D. A. and Whaley, K. B. [arXiv:quant-ph/0301032v1](https://arxiv.org/abs/quant-ph/0301032v1).
- [35] Doherty, A. C., Jacobs, K., and Jungmann, G. *Phys. Rev. A* **63**, 062306 (2001).
- [36] Viola, L., Lloyd, S., and Knill, E. *Phys. Rev. Lett.* **83**, 4888 (1999).
- [37] Buscemi, F., Chiribella, G., and D'Ariano, G. M. *Phys. Rev. Lett.* **95**, 090501 (2005).
- [38] Yu, T. and Eberly, J. H. *Phys. Rev. Lett.* **93**, 140404 (2004).
- [39] Dodd, P. J. and Halliwell, J. J. *Phys. Rev. A* **69**, 052105 (2004).

- [40] Tolkunov, D., Privman, V., and Aravind, P. K. *Phys. Rev. A* **71**, 060308 (2005).
- [41] Gong, Y.-X., Zhang, Y.-S., Dong, Y.-L., Niu, X.-L., Huang, Y.-F., and Guo, G.-C. *Phys. Rev. A* **78**, 042103 (2008).
- [42] Marek, P., Lee, J., and Kim, M. S. *Phys. Rev. A* **77**, 032302 (2008).
- [43] Paz, J. P. and Roncaglia, A. J. *Phys. Rev. Lett.* **100**, 220401 (2008).
- [44] Lopez, C., Romero, G., Lastra, F., Solano, E., and Retamal, J. C. *Phys. Rev. Lett.* **101**, 080503 (2008).
- [45] Cormick, C. and Paz, J. P. *Phys. Rev. A* **78**, 012357 (2008).
- [46] Almeida, M. P., deMelo, F., Hor-Meyll, M., Salles, A., Walborn, S. P., Ribeiro, P. H. S., and Davidovich, L. *Science* **316**, 579 (2007).
- [47] Laurat, J., Choi, K. S., Deng, H., Chou, C. W., and Kimble, H. J. *Phys. Rev. Lett.* **99**, 180504 (2007).
- [48] Kwiat, P. G., Barraza-Lopez, S., Stefanov, A., and Gisin, N. *Nature* **409**, 1014 (2001).
- [49] Pan, J. W., Gasparoni, S., Ursin, R., Weihs, G., and Zeilinger, A. *Nature* **423**, 417 (2003).
- [50] Peters, N. A., Altepeter, J. B., Branning, D., Jeffrey, E. R., Wei, T. C., and Kwiat, P. G. *Phys. Rev. Lett.* **92**, 133601 (2004).
- [51] Sainz, I. and Björk, G. *Phys. Rev. A* **77**, 052307 (2008).
- [52] Gavenda, M. and Filip, R. *Phys. Rev. A* **78**, 052322 (2008).
- [53] Gregoratti, M. and Werner, R. F. *J. Mod. Opt.* **50**, 915 (2003).
- [54] Cohen, O. *Phys. Rev. Lett.* **80**, 2493 (1998).
- [55] Yamamoto, N., Nurdin, H. I., James, M. R., and Petersen, I. R. *Phys. Rev. A* **78**, 042339 (2008).
- [56] Gordon, G. and Kurizki, G. *Phys. Rev. Lett.* **97**, 110503 (2006).
- [57] Maniscalco, S., Francica, F., Zaffino, R. L., Gullo, N. L., and Plastina, F. *Phys. Rev. Lett.* **100**, 090503 (2008).
- [58] Sciarrino, F., Nagali, E., Martini, F. D., Gavenda, M., and Filip, R. *Phys. Rev. A* **79**, 060304R (2009).
- [59] Gavenda, M., Filip, R., Nagali, E., Sciarrino, F., and Martini, F. D. *Phys. Rev. A* **81**, 022313 (2010).
- [60] Popp, M., Verstraete, F., Martin-Delgado, M. A., and Cirac, J. I. *Phys. Rev. A* **71**, 042306 (2005).

- [61] Yu, T. and Eberly, J. H. *Science* **323**, 598 (2009).
- [62] Blank, J., Exner, P., and Havlíček, M. *Lineární operátory v kvantové fyzice*, Univerzita Karlova Praha, Praha, (1993).
- [63] Verstraete, F., Dehaene, J., and DeMoor, B. *Phys. Rev. A* **64**, 010101R (2001).
- [64] Verstraete, F. and Wolf, M. M. *Phys. Rev. Lett.* **89**, 170401 (2002).
- [65] Bennett, C. H., DiVincenzo, D. P., Smolin, J. A., and Wootters, W. K. *Phys. Rev. A* **54**, 3824 (1996).
- [66] Bennett, C. H., Brassard, G., Popescu, S., Schumacher, B., Smolin, J. A., and Wootters, W. K. *Phys. Rev. Lett.* **76**, 722 (1996).
- [67] Deutsch, D., Ekert, A., Jozsa, R., Macchiavello, C., Popescu, S., and Sanpera, A. *Phys. Rev. Lett.* **77**, 2818 (1996).
- [68] Dehaene, J., denNest, M. V., DeMoor, B., and Verstraete, F. *Phys. Rev. A* **67**, 022310 (2003).
- [69] Peres, A. *Phys. Rev. Lett.* **77**, 1413 (1996).
- [70] Horodecki, M., Horodecki, P., and Horodecki, R. *Phys. Lett. A* **223**, 1–8 (1996).
- [71] Terhal, B. M. *Phys. Lett. A* **271**, 319 (2000).
- [72] Masanes, L. [arXiv:quant-ph/0510188](https://arxiv.org/abs/quant-ph/0510188).
- [73] R. Horodecki, P. H. and Horodecki, M. *Phys. Lett. A* **200**, 340 (1995).
- [74] Werner, R. *Phys. Rev. A* **40**, 4277 (1989).
- [75] Filip, R., Gavenda, M., Soubusta, J., Černoč, A., and Dušek, M. *Phys. Rev. Lett.* **93**, 180404 (2004).
- [76] Plenio, M. B. and Virmani, S. [arXiv:quant-ph/0504163](https://arxiv.org/abs/quant-ph/0504163).
- [77] Wootters, W. K. *Phys. Rev. Lett.* **80**, 2245 (1998).
- [78] Horodecki, R., Horodecki, P., Horodecki, M., and Horodecki, K. [arXiv:quant-ph/0702225](https://arxiv.org/abs/quant-ph/0702225).
- [79] Horodecki, M., Horodecki, P., and Horodecki, R. *Phys. Rev. Lett.* **78**, 574 (1997).
- [80] Horodecki, M., Shor, P. W., and Ruskai, M.-B. *Rev. Math. Phys.* **15**, 629 (2003).
- [81] Ruskai, M.-B. *Rev. Math. Phys.* **15**, 643 (2003).
- [82] <http://www.ise.ncsu.edu/mirage/GAToolBox/gaot>.

- [83] <http://www.ft.utb.cz/people/zelinka/soma/>.
- [84] Yu, T. and Eberly, J. H. *Opt. Comm.* **264**, 393 (2006).
- [85] Yu, T. and Eberly, J. H. *Quantum Information and Computation* **7**, 459 (2007).
- [86] Hayashi, H., Kimura, G., and Ota, Y. *Phys. Rev. A* **67**, 062109 (2003).
- [87] Horodecki, M., Horodecki, P., and Horodecki, R. *Phys. Rev. A* **60**, 1888 (1999).
- [88] Kent, A., Linden, N., and Massar, S. *Phys. Rev. Lett.* **83**, 2656 (1999).
- [89] Wang, Z.-W., Zhou, X.-F., Huang, Y.-F., Zhang, Y.-S., Ren, X.-F., and Guo, G.-C. *Phys. Rev. Lett.* **96**, 220505 (2006).
- [90] Kraus, K. *States, Effect, and Operations: Fundamental Notions in Quantum Theory*, Springer-Verlag, Berlin, (1983).
- [91] Scully, M. and Zubairy, M. *Quantum Optics*, Cambridge University Press, Cambridge, (1997).
- [92] Zhao, Z., Yang, T., Chen, Y. A., Zhang, A. N., and Pan, J. W. *Phys. Rev. Lett.* **90**, 207901 (2003).
- [93] Walther, P., Resch, K. J., Brukner, ., Steinberg, A. M., Pan, J. W., and Zeilinger, A. *Phys. Rev. Lett.* **94**, 040504 (2005).
- [94] DiVincenzo, D. P. *Lecture Notes in Computer Science*, Springer-Verlag, Berlin, (1999).
- [95] Verstraete, F., Popp, M., and Cirac, J. *Phys. Rev. Lett.* **92**, 027901 (2004).
- [96] Smolin, J. A., Verstraete, F., and Winter, A. *Phys. Rev. A* **72**, 052317 (2005).
- [97] Gour, G. and Spekkens, R. *Phys. Rev. A* **73**, 062331 (2006).
- [98] Linden, N., Massar, S., and Popescu, S. *Phys. Rev. Lett.* **81**, 3279 (1998).
- [99] Verstraete, F., Audenaert, K., Bie, T. D., and Moor, B. D. *Phys. Rev. A* **64**, 012316 (2001).
- [100] Ishizaka, S. and Hiroshima, T. *Phys. Rev. A* **62**, 022310 (2000).
- [101] Wei, T. C., Nemoto, K., Goldbart, P. M., Kwiat, P. G., Munro, W. J., and Verstraete, F. *Phys. Rev. A* **67**, 022110 (2003).
- [102] Cinelli, C., Nepi, G. D., Martini, F. D., Barbieri, M., and Mataloni, P. *Phys. Rev. A* **70**, 022321 (2004).
- [103] Sciarrino, F., Sias, C., Ricci, M., and Martini, F. D. *Phys. Rev. A* **70**, 052305 (2004).

- [104] Ghotbi, M., Ebrahim-Zadeh, M., Majchrowski, A., Michalski, E., and Kityk, I. *Optics Letters* **29**, 21 (2004).
- [105] James, D. F. V., Kwiat, P., Munro, W. J., and White, A. G. *Phys. Rev. A* **64**, 052312 (2001).
- [106] Hong, C. K., Ou, Z. Y., and Mandel, L. *Phys. Rev. Lett.* **59**, 2044 (1987).
- [107] Zou, X. Y., Wang, L. J., and Mandel, L. *Phys. Rev. Lett.* **67**, 318 (1991).
- [108] Englert, B. G. *Phys. Rev. Lett.* **77**, 2154 (1996).
- [109] Scully, M. O., Englert, B. G., and Walther, H. *Nature* **351**, 111 (1991).
- [110] Tittel, W., Brendel, J., Gisin, N., and Zbinden, H. *Phys. Rev. A* **59**, 4150 (1999).